

Duquesne University

Duquesne Scholarship Collection

Electronic Theses and Dissertations

Spring 5-8-2021

Machine Learning Applied to Colloidal Properties of Perfluorocarbon Nanoemulsions for Imaging in ARDS/ALI

Marco Hosfeld

Follow this and additional works at: <https://dsc.duq.edu/etd>



Part of the [Biomaterials Commons](#), [Complex Mixtures Commons](#), [Nanomedicine Commons](#), [Other Biomedical Engineering and Bioengineering Commons](#), and the [Pharmaceutical Preparations Commons](#)

Recommended Citation

Hosfeld, M. (2021). Machine Learning Applied to Colloidal Properties of Perfluorocarbon Nanoemulsions for Imaging in ARDS/ALI (Master's thesis, Duquesne University). Retrieved from <https://dsc.duq.edu/etd/1978>

This One-year Embargo is brought to you for free and open access by Duquesne Scholarship Collection. It has been accepted for inclusion in Electronic Theses and Dissertations by an authorized administrator of Duquesne Scholarship Collection.

MACHINE LEARNING APPLIED TO COLLOIDAL PROPERTIES OF
PERFLUOROCARBON NANOEMULSIONS FOR IMAGING IN ARDS/ALI

A Thesis

Submitted to the Rangos School of Health Sciences

Duquesne University

In partial fulfillment of the requirements for
the degree of Master of Science

By

Marco Hosfeld

May 2021

Copyright by
Marco Hosfeld

2021

MACHINE LEARNING APPLIED TO COLLOIDAL PROPERTIES OF
PERFLUOROCARBON NANOEMULSIONS FOR IMAGING IN ARDS/ALI

By

Marco Hosfeld

Approved March 22, 2021

Dr. Jelena Janjic
Associate Professor of Pharmacy
(Committee Chair)

Dr. John Viator
Professor of Biomedical Engineering
(Committee Member)

Dr. Kimberly Williams
Associate Professor of Biomedical
Engineering
(Committee Member)

Dr. Lauren Sugden
Assistant Professor of Statistics
(Reader)

Dr. Fevzi Akinci
Dean, Rangos School of Health Sciences

Dr. John Viator
Chair, Engineering
Professor of Biomedical Engineering

ABSTRACT

MACHINE LEARNING APPLIED TO COLLOIDAL PROPERTIES OF PERFLUOROCARBON NANOEMULSIONS FOR IMAGING IN ARDS/ALI

By

Marco Hosfeld

May 2021

Dissertation supervised by Dr. Jelena Janjic

Acute Respiratory distress Syndrome (ARDS) and Acute Lung Injury (ALI) are inflammatory lung pathologies consisting of non-hydrostatic pulmonary edema leading to hypoxia and impaired gas exchange in the lungs. ARDS/ALI is both difficult to study and treat as it is not in itself a specific pathology but rather a syndrome consisting of many pathologies that vary case by case. It is, however, consistently characterized by an explosive acute inflammatory response in the lung parenchyma leading to the ultimate hypoxia and impaired gas exchange that characterizes ARDS/ALI. Although time has seen to an increase in the understanding of ARDS/ALI, the mortality rate remains in the range of 30-50%. For these reasons, nanomedicine may offer solutions to the diagnosis and treatment of ARDS/ALI. Nanomedicine, by definition, utilizes nanoscale materials to address various disease states in the hopes of being more effective

than traditional medicine. Especially in cases of imaging, nanomedicine seeks to redress some of the issues seen in traditional imaging such as with more targeted delivery platform. In ARDS imaging, such as CT and MRI, has been used to confirm the condition through pulmonary opacification, however, specific tracking of macrophages using MRI has only been tentatively explored. This can be achieved through macrophage targeted nanomedicine platforms, therefore focus of this paper will be on macrophage targeted perfluorocarbon(PFC) nanoemulsions. We believe that nanoemulsions aimed for macrophage imaging in severely ill patients require the highest quality possible. We will understand the current state of the art through machine learning to determine what manufacturing parameters impact the performance of perfluorinated Nanoemulsions. Machine learning will be used to analyze what parameters of production are critical to the various colloidal attributes (size, zeta potential, and PDI) to the performance of emulsion-based drug delivery platforms.

TABLE OF CONTENTS

| | Page |
|---|------|
| Abstract | iv |
| ARDS/ALI, inflammation, and Immune Cell Tracking | 1 |
| Epidemiology and Risk Factors..... | 2 |
| Pathophysiology | 3 |
| Treatment of ARDS/ALI | 5 |
| Immune Cell tracking and Inflammation in ARDS/ALI | 6 |
| Nanomedicine Systems..... | 8 |
| Nanomedicine Systems in General..... | 9 |
| Fullerenes | 9 |
| Lipid Based NPs | 10 |
| Micelles..... | 11 |
| Quantum Dots..... | 12 |
| Polymeric NPs | 12 |
| Dendrimers..... | 14 |
| Composite Nanostructures..... | 14 |
| Emulsions(micro/nanoemulsions)..... | 14 |
| Liposomes..... | 15 |
| Nanomedicine Systems as Treatment for ARDS/ALI | 16 |
| Examples..... | 16 |
| fullerenes..... | 16 |
| Liposomes..... | 17 |

| | |
|---|----|
| Emulsions..... | 18 |
| PFC Nanoemulsions for Immune Cell Imaging | 19 |
| Micelles..... | 22 |
| Polymeric NPs | 23 |
| Lipid Based NPs | 23 |
| Quantum Dots | 24 |
| Tuning of Nanomedicines for Pulmonary Applications | 25 |
| Nanomedicine Size..... | 25 |
| Nanomedicine Shape..... | 27 |
| Surface Properties..... | 28 |
| Metanalysis of Reported Nanoemulsions using Machine Learning..... | 29 |
| Introduction to Machine Learning..... | 30 |
| Colloidal Properties of Nanoemulsions and Machine Learnin..... | 31 |
| Methods..... | 34 |
| Data Collection Process | 34 |
| Data Preparation Process | 35 |
| Machine Learning Analysis | 36 |
| Analysis of Model and Generated Data | 39 |
| Predictions and Validation..... | 39 |
| Results | 40 |
| Conclusion | 45 |

LIST OF FIGURES

| | Page |
|------------------|------|
| Figure 1 | 32 |
| Figure 2 | 33 |
| Figure 3 | 36 |
| Figure 4 | 38 |
| Figure 5 | 40 |
| Figure 6 | 43 |
| Figure 7 | 45 |
| Figure S1 | 47 |
| Figure S2 | 48 |
| Figure S3 | 49 |
| Figure S4 | 50 |
| Figure S5 | 51 |
| Figure S6 | 52 |
| Figure S7 | 53 |
| Figure S8 | 54 |
| Figure S9 | 55 |
| Figure S10 | 56 |
| Figure S11 | 57 |
| Figure S12 | 58 |
| Figure S13 | 59 |
| Figure S14 | 60 |

| | |
|------------------|----|
| Figure S15 | 61 |
| Figure S16 | 62 |

ARDS/ALI, Inflammation, and Immune Cell Tracking

Acute Respiratory Distress Syndrome (ARDS) and Acute Lung Injury (ALI), of which ARDS is an extreme form, are life threatening disease states often present in critically ill patients.¹ It is a common cause of respiratory failure in critically ill patients and is defined by acute onset of noncardiogenic pulmonary edema, hypoxemia, and, as is often the case, the need for mechanical ventilation.² ARDS occurs in instances of severe systemic inflammation and pulmonary trauma/inflammation and presents itself in ~10% of all patients in ICUs worldwide. Despite improvements to the treatment of the condition, mortality remains high at 30-40% in most studies. Mechanical ventilation is critical in the clinical setting to treat ARDS, however, if performed improperly can result in further damage to the lungs thereby leading to a form of ARDS/ALI known as ventilatory associated lung injury (VALI).¹

ARDS was initially defined in 1967 with a case-based report that described the clinical presentation in critically ill adults and children of acute hypoxemia, noncardiogenic pulmonary edema, reduced lung compliance, increased work of breathing, and the need for positive pressure ventilation in association with several clinical disorder defined by trauma and inflammation in the patient.² A criteria was set for defining the syndrome known as the Berlin definition.³ Depending on the level of blood oxygenation, ARDS can be categorized as ‘mild’, ‘moderate’, and ‘severe’. The diagnosis of ARDS depends on clinical criteria alone as it is not practical to obtain pathological samples of lung tissue in most patients.

The 2012 berlin definition³ of ARDS consists of four primary criteria: timing, origin, imaging, and oxygenation. With regard to timing, respiratory failure must occur within one week of the known insult or new/worsening respiratory conditions. The origin must not be fully explained by cardiac function or volume overload. Imaging must indicate bilateral opacities on

chest radiograph or CT that is not fully explained by effusion, collapse, or nodules. Finally, it is graded by oxygenation as being mild to severe depending on PaO₂/FiO₂ level (201–300 mmHg, 101-200 mmHg, and ≤100 mmHg for each case respectively).

Epidemiology and Risk Factors

It is estimated there is an annual incidence of 190,000 cases of ARDS in the United States with a hospital mortality of 38.5%.⁴ In another study the prevalence of ARDS in ICUs worldwide was found to be 10% and ARDS was identified in 23% of all ventilated patients.⁵ The same study reported that hospital mortality rate was 34.9% for patients with mild ARDS, 40% for moderate ARDS, and 46.1% for patients with severe ARDs. The actual rate, however, remains unclear regarding how much of the reported mortality can be attributed to ARDS alone or the underlying conditions associated with ARDS. For example, a follow up analysis of the same study found that immunocompromised patients experienced a mortality rate of 52% as compared to non-immunocompromised patients who experienced a mortality rate of 36%.⁶

Several comorbidities and exposures have been associated with increase susceptibility to ARDS, including alcohol abuse, smoking, air pollution, and low blood albumin levels.² Diabetes on the other hand has been associated with a lower risk of ARDS development for reasons that remain unclear. Furthermore, transfusion related acute lung injury (TRALI) can also lead to ARDS. Major risk factors for developing this condition include recent liver surgery, chronic alcohol abuse, current smoking, higher peak airway pressure (highest airway pressure while being ventilated) and positive fluid balance.⁷ In addition, ARDS has been reported to have a higher mortality among black and Hispanic patients than white patients. There are even differences among men and women, wherein, men have, on average, higher mortality rates than women.²

Pathophysiology

A normal lung is structured to facilitate carbon dioxide-oxygen gas exchange across each alveolar capillary unit. The selective barrier to fluid and solutes in the lung is established by a single layer of endothelial cells. The surface of this alveolar epithelium is lined by alveolar type I and type II cell, thereby forming a tight barrier that allows for primarily the diffusion of oxygen and carbon dioxide to take place. The alveolar type II cells secrete surfactant, while both alveolar type I and II cells have the capacity to absorb excess fluid from the airspace. Once edematous fluid is absorbed into the lung interstitium the fluid can be removed by the lymphatic system and lung microcirculation. The cellular makeup of a normal alveolus also includes alveolar macrophages but not neutrophils. Alveolar macrophages, neutrophils, and other immune cells however, are critical in the defense of a normal lung and are key in ARDS/ALI.

In ARDS, there is increased permeability to liquid and protein across the lung endothelium, which then leads to edema of the lung interstitium. Next the edematous fluid is transported to the alveoli via injury to the normally tight barrier properties of the alveolar epithelium. The increased alveolar-capillary permeability results in the accumulation of fluid in the alveolar space. This leads to impaired gas exchange.

Interstitial and alveolar edema are key features of diffuse alveolar damage (DAD) in the acute exudative phase of ARDS. Eosinophilic depositions termed hyaline membranes are also a defining features of DAD and a histopathological hallmark of ARDS.² Other findings include alveolar hemorrhage, the accumulation of neutrophils, fibrin deposition, and alveolar collapse. After the exudative phase of the syndrome. After the exudative phase, alveolar type II cell hyperplasia occurs in the proliferative phase. Interstitial fibrosis can occur in this phase. In what

is known as the fibrotic phase. However, DAD is only present within a subset of ARDS patients with pathological heterogeneity evident.

Fundamentally, ARDS is characterized by injury to the alveolar capillary unit consisting of three overlapping phases: the exudative, proliferative, and the fibrotic phases.⁸ The exudative phase starts within 48 hours and lasts for about a week. Pathological features of this stage include capillary congestion, fibrin rich microthrombus formation, interstitial and alveolar edema, intra-alveolar hemorrhage, and hyaline membranes (made of plasma proteins and cellular debris) lining the alveoli and alveolar ducts. There is extensive necrotic death of alveolar type I cells and irregular endothelial changes. Increasing numbers of neutrophils are found in capillaries and interstitial tissues, and within airspaces. The proliferative phase starts roughly at the end of the first week. It is characterized by organization of exudates and by fibrosis. There is proliferation of alveolar type II cells into alveolar type I cells and fibroblasts. Destruction of the pulmonary capillary bed may lead to pulmonary hypertension and eventually to right ventricular failure. Persistent hypoxemia, increased alveolar dead space, and an additional decrease in lung compliance are clinically evident. The final, fibrotic phase is characterized by increased collagen deposition and increased fibrosis of the lungs.

The actual mechanisms of lung injury are the responsibility of the explosive acute inflammatory response in the lung parenchyma. The inflammatory response involves the recruitment of blood leukocytes and the activation of tissue macrophages along with the production of various mediators. The consequences of which are endothelial disruption with increased alveolar capillary permeability along with the host of other conditions mentioned prior. Neutrophils predominate histological specimens and are present in the edematous fluid of the lungs in ARDS. These cells release toxic bioactive mediators damaging the endothelial cells with

increased vascular permeability leading to hemorrhage and parenchymal injury. While neutrophils may play a central role in lung injury macrophages too have been shown to release proinflammatory cytokines. They may also be important mediators not only in initiating the inflammatory response, but also in regulation of fibroblast function in later stages of ARDS.⁸

Treatment of ARDS/ALI

Treatment of ARDS is generally supportive in nature with an emphasis on treating the underlying cause of the disease such as mechanical ventilation⁹ and corticosteroid administration¹⁰. As a result, the primary focus of this section will be on the delivery of corticosteroids and other anti-inflammatory agents. There are of course some exceptions, such as dimethyl silicone¹¹, but the majority of agents that can be optimized for nanomedicine use in ARDS/ALI will consist of anti-inflammatory agents.

Inflammation is a critical factor in the pathophysiology of ARDS irrespective of the root cause of the condition. Additionally, in the inflammatory cascade insufficient glucocorticoid receptor-mediated inhibition of NF- κ B is thought to be central to ARDS pathogenesis.¹² While some patients experience rapid resolution of the disorder, persistent ARDS is characterized by ongoing inflammation.^{13,14}

Currently there are no pharmacological protocols effective in treatment of the condition¹⁵. However, there have been multiple agents considered for modifying the progression of ARDS such as surfactants,¹⁶ inhaled nitric oxide,¹⁷ antifungal drugs,¹⁸ and N-acetyl cysteine.¹⁹ Corticosteroids have also been found to show favorable results in some studies and no benefits in others. These therapeutic agents, however, have several adverse effects.²⁰ Another class of drugs that may be useful in the pharmacological treatment of ARDS is antioxidants. Reactive oxygen species have been implicated in the pathophysiology of ARDS;

specifically the increased pulmonary-capillary permeability.²¹⁻²⁴ Furthermore, antioxidants have been used in previous studies of ARDS.²⁵ while the effects of such treatment are up for debate, antioxidants have been heavily explored with regards to their potential therapeutic use in ARDS. Nanomedicine is useful in both these medications and others, especially in the treatment of ARDS. The purpose of nanomedicine is to enhance drug efficacy while reducing off target effects. This is critical in ARDS/ALI, where the pharmacological treatments have questionable efficacy. Maximizing potential therapeutic effects while minimizing off target effects will be key to developing a potent and effective pharmaceutically based therapy for ARDS/ALI.

Immune Cell Tracking and Inflammation in ARDS/ALI

Inflammation is an integral part of ARDS/ALI. The syndrome is characterized by an explosive acute inflammatory response in the lung parenchyma.⁸ This ultimately leads to alveolar oedema, decreased lung compliance, and inevitably hypoxemia.² This integral relationship between inflammation and ARDS/ALI can be seen in the relationship between secondary insults and their ability to cause ARDS. Generally speaking, these insults can be broken down as primary and secondary. Primary insults are characterized by the direct injury of the lungs. Secondary insults on the other hand are characterized by widespread systemic inflammation such as sepsis. Sepsis is the most common risk factor in ARDS.⁸ In fact the presence of Interleukin 8 (IL-8) in the bronchoalveolar lavage is used to predict the development of ARDS in trauma patients.²⁶ As IL-8 is also known as neutrophil chemotactic factor, it is readily apparent that it plays a role in mediating inflammatory effects of the immune system. As ARDS is a highly inflammatory syndrome it is critical to understand inflammatory progression prior to and in patients at high risk for condition. As such imaging techniques that provide non-invasive, early, and specific diagnostic information is desirable and helpful in such patients.

In order to track immune cells within patients, in real time, a method by which modern imaging techniques can be applied is highly desirable. In this case tracer agents such as ^{19}F Fluorine MRI. The signal used for MRI can be derived directly from fluorinated molecules such as ^{19}F .²⁷⁻³⁰ When the subject is placed in a magnetic field there is a magnetic moment associated with ^{19}F that tends to align along the direction of the magnetic field. The ^{19}F nuclei can be perturbed from this equilibrium by pulsating radio frequency radiation. Following the removal of the radio frequency signal the nuclei recover to equilibrium thereby inducing a transient voltage on a receiving antenna. This voltage constitutes a nuclear magnetic resonance (NMR) signal.²⁷

The physical principles behind both ^1H (traditional) MRI and ^{19}F MRI are the same, however, as opposed to metal ion based contrast agents the ^{19}F agent acts more like a probe wherein they can be directly detected and measured via Fluorine MRI. It does not require any background signal. The ^{19}F signal is directly proportional to the number of fluorine atoms and the number of labeled cells present. This implies it is actually possible to quantify the degree of signal and thereby quantify the degree of inflammation in the case of labeled immune cells.

It is possible to label cells for Fluorine MRI detection via the use of perfluorocarbon (PFC) nanoemulsions. While this section will focus on this topic as well, there will be a following section to deal more specifically with PFC nanoemulsions. PFC based cell tracking allows for a high degree of specificity in cell detection and the quantification of cells. As previously discussed, this is related to the Fluorine MRI detecting the ^{19}F atomic nuclei directly and its function as a tracer agent as opposed to a contrast agent. Furthermore, because of the low concentrations of naturally occurring ^{19}F in the body, there is negligible background signal from host tissues. However, pure PFC cannot be taken up by cells. PFC must be formulated as a nano or microemulsion for it to be taken up by cells.³¹ This can either be done *in vivo* or *ex vivo*.

As a result of all the factors discussed previously, PFC nanoemulsion are therefore a good method to track cells non-invasively. As emulsified PFCs are preferentially phagocytized by monocytes/macrophages,²⁸ these cells are easily imaged and thereby inflammation can be easily imaged. In particular the inflammation of the lungs has been imaged before using emulsified PFC formulations.²⁸ In this particular study inflammation was induced in mice via intratracheal instillation of LPS followed by intravenous injection of PFCs. While there was no evidence of lung injury using traditional MRI, concurrent ¹⁹F images clearly show PFC accumulation in both pulmonary lobes. It was only after 48 hours pos LPS instillation that traditional MRI signal revealed damage.²⁸ Additional experiments with varying doses of LPS indicated that ¹⁹F signal intensity correlates strongly to the amount of LPS used in instillation and therefore the severity of pulmonary trauma.

Nanomedicine Systems

Nanomedicine is defined as the application of nanobiotechnology to medicine.³² Nanomedicine and drug delivery nanosystems specifically, are highly promising vehicles for both highly efficient and highly targeted delivery of therapeutic agents.³³ For instances, a single dose of nanoemulsion carrying celecoxib can reduce total body burden of drug by over 2000 fold as compared to oral delivery.³⁴ In this section, we will cover a variety of these nanomedicine systems with a specific focus on aspects of drug loading and functionalization methods. Furthermore, we will cover specific examples of nanomedicine systems with respect to ARDS/ALI.

Nanomedicine Systems in General

Fullerenes

Fullerenes are molecules composed entirely of carbon in the form of a hollow sphere, ellipsoid, or tube.³⁵ More broadly one can view this as a molecule consisting entirely of carbon in the form of a closed or partially closed mesh. Fullerenes show wide availability due to their small size and ability to be functionalized. While not themselves used in pulmonary medicine, other carbon based nanoparticles have been used in other applications. There are some toxicity concerns in pulmonary applications, however, those will be discussed in a later section. Their inclusion here is a result of their spheroid shape and similarity to other carbon based NPs. Drug loading of fullerenes is dependent on its structural features. Drugs are often conjugated to the fullerene molecule. In this fashion, the functionalization of Fullerenes can be used to load drugs. The relatively high number of double bonds allow for a high degree of functionalization through conjugation of various molecules.³⁶ Functionalization is necessary before fullerenes can be used for drug delivery. The extreme hydrophobic character of the molecules contributes to this, and the addition of hydrophilic moieties are necessary to overcome this.³⁵ Their ability to form a variety of derivative molecules through conjugation is core to their ability to deliver various payloads. As long as a molecule can be conjugated to a fullerene it is possible to use them modify the molecules characteristics as a whole. This gives a high degree of flexibility to fullerenes as delivery vehicles. It should be noted that this is a chemical modification to the molecule and, given the number of carbon-carbon double bonds, may be difficult to control with precision.

Lipid Based NPs

Solid Lipid NPs (SLNs) are colloidal based drug delivery system composed of lipids that remain solid at both room and body temperature. Solid lipid forms a matrix material for drug encapsulation while it is stabilized by surfactant/polymers.³⁷ SLNs have significant advantages in long term physical stability, controlled release of both hydrophilic and lipophilic drug, low toxicity, low cost, and site specific targeting.³⁸ With regard to drug delivery, there are three primary drug incorporation models useful in drug loading of SLNs: homogenous matrix, drug enriched shell, and drug enriched core models. In the homogenous matrix model, drug is dispersed in the lipid core and are usually highly lipophilic. The other models (core and shell) are driven by precipitation and phase separation, respectively. The drug is concentrated in the core and shell respectively.³⁹ There are also other methods to manufacture SLNs that allow for incorporation of hydrophilic drugs by taking advantage of phase separation.⁴⁰ With regards to functionalization, As SLNs are an emulsion based nanomedicine system it is possible to functionalize them through modification of the surfactant molecules that make up the nanoparticle. It is possible to functionalize SLNs with a variety molecules. SLNs have been chemically functionalized using mannose has been used to target alveolar macrophages.⁴¹

Nanostructured Lipid Carriers (NLCs) are the second generation of lipid based nanocarrier. They were developed to overcome some of the limitations associated with NLPs. As such, NLCs have higher drug loading capacity and avoid drug expulsion as a result of lipid crystallization. NLCs are composed of a mix of solid and liquid lipids.^{37,38,42} With regards to drug loading, NLCs were designed to overcome loading issues associated with SLNs. By utilizing a combination of liquid and solid lipid, NLCs avoid drug expulsion by crystallization through the creation of liquid imperfections in the matrix.³⁷ This is done through the creation of three types of NLCs:

Imperfect, structureless, and mixed type.^{37,42} Each of these varieties increase loading capacity though the introduction of features in the solid lipid matrix that allow for drug to be loaded more efficiently than in SLNs. With regards to functionalization, NLCs have been subject to various modifications to enhance their drug delivering properties. For instance, cysteine has been bound to the polymer surfactant in an NLC blend to facilitate intestinal transport of docetaxel.⁴³ In another instance, NLCs underwent surface modification for the inclusion of a glycol chitosan for brain delivery.⁴⁴

Micelles

Micelles are a colloid formed by a surfactant in equilibrium with the molecules that contribute at micelle formation.⁴⁵ By the definition, while similar to emulsions, micelles are not emulsions and should be treated as such. Furthermore, this section will deal primarily with polymeric Micelles in order to highlight some of differences between them and emulsions. Polymeric micelles are nanoscopic core-shell structures formed by amphiphilic polymers.⁴⁶ Based on the forces of assembly, these micelles can be divided into several categories: Hydrophobically assembled, polyion-complex micelles, and micelles stemming from metal complexation.⁴⁷ With regards to drug loading of polymeric micelles typically drug loading occurs via entrapment in the micelle.³² these drugs are contained within the micellar core and protected by the polymers.⁴⁶ With regards to functionalization, functional groups displayed on the surface of the micelle are incorporated within the polymer chains themselves.⁴⁸ Properties can also be altered with the shape of the micelle. Wormlike micellar structures have been shown to have a circulation time ten times longer than their spherical counterparts.⁴⁹ These modes of functionalization can create pH responsive micelles³² and targeted micelles.⁴⁷

Quantum Dots

Quantum dots are nanoscale semiconductor structures with very unusual properties.⁵⁰ Quantum Dot nanomedicine systems for drug delivery have the possibility of improving drug stability, circulation time, targeting, and distribution.⁵¹ This can be considered a result of three properties of Quantum Dots: size dependent optical and electronic properties, water solubility, and ability to be conjugated with biological molecules.⁵² The most distinctive property of Quantum Dots is their size dependent fluorescent emissions ranging from Near UV to Near IR. These optical properties make them ideal candidates as luminescent nano-probes.⁵¹ As Quantum Dots are solid particle structures, the only way to ensure drug delivery and functionalization is through surface modification.

Polymeric NPs

Polymeric NPs have numerous advantages over other varieties of NPs including: modified surface properties, high encapsulation efficiency, prolonged drug delivery, and a long shelf life.⁵³ The surface and chemical properties of the NPs are modified to make them biodegradable.^{54,55} These properties of polymeric nanoparticles ensure that they can effectively deliver drug, have a high degree of biocompatibility, and have limited toxicity. Synthetic Polymer NPs include NPs of PLA, PLGA, and PCL. PLA and PLGA were developed for use in surgical implants and tissue repair and have been widely used for various biomedical applications including drug delivery.⁵⁶ Furthermore, PLA and PLGA have been used extensively in drug delivery due to their highly tunable biodegradability and mechanical properties.^{57,58} Additionally, PCL beads have been used for the controlled release and targeted drug delivery.⁵⁹ With regards to drug loading, there are a variety of loading methods to incorporate drug into synthetic polymeric NPs and these can vary heavily by type of polymer. Here we will focus on PLA NPs and methods broadly applicable to

other polymers. Broadly speaking, there are four methods to PLA NP production: emulsion methods, precipitation methods, direct composition, and cutting-edge methods.⁵⁶ These methods can be applied to all varieties of synthetic polymers and through these methods drug can either be encapsulated by NP or incorporated in its matrix. With regards to functionalization, polymeric nanoparticles easily undergo surface modification.⁶⁰ Furthermore, both bulk and surface properties can undergo modification relatively simply through: blending of different polymers, coating, copolymerization, cross linking, entrapment, etc.⁵⁶ There is a huge diversity of methods to functionalize polymeric NPs and these modifications dramatically alter behavior and favorably enhance therapeutic efficacy.⁶¹ In addition to synthetic polymers there are natural polymer NPs (Alginate, Chitosan, Gelatin). Natural polymers such as gelatin, for instance, are biodegradable, biocompatible, and covalently bind active compounds.⁶² Chitosan is a mucoadhesive and permeation enhancer; helping facilitate retention in the lungs following administration.⁶³ Alginate is another polymer with high biocompatibility and a hydrophilic matrix for efficient drug loading.⁶⁴ Natural polymers have their own unique advantages that can make them an attractive alternative to synthetic polymeric NPs. With regards to, it should be noted that generally speaking natural polymers are hydrophilic while synthetic polymers are hydrophobic.⁶⁵ Furthermore, natural polymers tend to display fast and uncontrolled release profiles.⁶⁶ With regards to functionalization, Natural polymers can be subjected to similar chemical treatments as synthetic polymers. Given some of the unique properties of natural polymers, however, not all surface modification treatments used with synthetic polymers are useful or necessary.

Dendrimers

Dendrimers are repetitively branched molecules defined by a central core, and interior branching structure, and an exterior with functional surface groups.⁶⁷ they have shown their potential abilities to entrap or conjugating useful molecules and drugs for functionalization and drug delivery respectively.⁶⁸ furthermore, the high water solubility, biocompatibility, and precise molecular weight of dendrimers (as compared to traditional polymers) make them ideal for drug delivery.^{69–71} While highly interesting, they are somewhat impractical as an effective scale up process has yet to be discovered.⁷² With regards to drug loading, two primary strategies are used to load drugs into dendrimers: “complexation” by encapsulation/electrostatic binding by ionic groups at the dendrimer periphery and “conjugation” by covalent bonding to dendrimer.⁷³ Optimizing size and surface properties can optimize dendritic delivery platforms for different modes of delivery.⁶⁸ With regards to functionalization, the actual structure of dendrimers lend themselves rather easily to functionalization. The precise control over each step of polymerization in dendrimers leads to an unprecedented degree of control. Functionalization comes easily by modification of the terminal end groups. For instance, amine terminated PAMAM dendrimers cross biological membranes via paracellular and endocytotic pathways.⁷⁴ Other modifications lead to different results.

Composite Nanostructures

Nano and Microemulsions

Emulsions are colloidal dispersions in which the dispersed phase and the medium are both liquid. In essence, they consist of liquid droplets suspended in a liquid medium. Within the field of emulsions, we must distinguish between nano and microemulsions. Microemulsions are clear, thermodynamically stable dispersions stabilized by an interfacial surfactant layer.⁷⁵

Nanoemulsions, on the other hand, are kinetically stable⁷⁶ and are therefore less stable than microemulsions. With regards to drug loading of emulsions, drug loading is heavily dependent on the dispersed phase(s) contained within the nano/microemulsion droplets. Oils phases which have high drug loading capabilities are generally used in their development.⁷⁷ Furthermore, other dispersed phases can be used. Perfluorocarbons, for instance, have been used in oxygen delivery.⁷⁸ In fact a combination of dispersed phases can be used to generate a multiphasic emulsion, such as a triphasic emulsion.⁷⁹ Of course, even the dispersed phase can also be used as a drug. With regards to functionalization, as emulsions are surfactant stabilized systems it is possible to modify the surfactant used to functionalize the nano/microemulsion droplets.

Liposomes

Liposomes are nanosized vesicular structures consisting of an aqueous core surrounded by phospholipid layers.⁸⁰ They are the first nanosystem for drug delivery that has been successfully translated into real-time clinical applications with a well established ability to deliver a variety of payloads.⁸¹ They can be broadly broken down into unilamellar and multilamellar liposomes.⁸² Liposomes are highly useful in that they can both be functionalized in a variety of ways and the payload is contained in a controlled environment.⁸³ Principally, there exist unilamellar liposomes are liposomes consisting of a single phospholipid bilayer. With regards to drug loading, generally speaking the creation of liposomes involves four primary steps: drying lipid from organic solvent, dispersion in an aqueous phase, purification, and analysis.⁸² Generally speaking it is the aqueous phase that typically holds the drug, however, lipophilic drugs can be incorporated into the phospholipid layers of the liposome. With regards to functionalization one of the most common methods of functionalizing liposomes is the creation of stealth liposomes. By coating liposomes in PEG to reduce percentage of uptake by macrophages they can evade the

immune system longer for prolonged circulation.^{81,82} different methods of functionalization can impart enhanced stability, drug targeting, and other physical/chemical characteristics.⁸⁴ Furthermore, there exist multilamellar structures have an onion like architecture in which phospholipid bilayers are nested within one another. Each layer is separated by layers of aqueous phase.

Nanomedicine Systems for Treatment of ARDS/ALI

ARDS is a form of hypoxemic respiratory failure characterized by severe impairment in gas exchange and lung mechanics. ALI is term used in animal models categorized as a milder form of the human ARDS.⁸⁵ Current treatment measures aim to modulate inflammation or its consequences in ARDS patients and current therapies include: corticosteroids,⁸⁶ neutrophil elastase inhibitors,⁸⁷ granulocyte-macrophage colony stimulating factor,⁸⁸ statins,⁸⁹ omega-3 fatty acids,⁹⁰ surfactant,¹⁶ inhaled β agonists,⁹¹ nitric oxide therapies,⁹² and neuromuscular blockers.⁹³ It is along these lines that nanomedicine works. It enhances the efficiency of drug targeting and drug delivery. In ARDS/ALI, this means that therapeutic agents are delivered more efficiently and effectively to their targets

Example Nanomedicine Systems

Fullerenes

While the primary object of focus will be fullerenes, the discussion will be centered on carbon-based NPs as a whole as a result of their highly inclusive geometry. Fullerenes are taken as representative of carbon-based NPs. It must be understood that carbon based NPs have high pulmonary toxicity.^{94,95} This, however, should not preclude the possibility of their use in the future. The degree of toxicity is highly variable depending on the form of the carbon NP.^{96,97} Furthermore, the geometry itself is not necessarily toxic.⁹⁸ Distinct Structural properties of

carbon NPs such as propensity for functional modification and potential biocompatibility⁹⁹ mean that they cannot be ignored as potential nanomedicine system for ARDS/ALI.

Carbon NP toxicity induces a host of pathological responses, chief of which are inflammatory responses and fibrogenic responses.^{94,100} In order to overcome this, a study created biologically inspired rosette nanotubes. While this study did not look at carbon nanotubes they did look at nanotubes in general. This work suggests that nanostructures with a biological design may mitigate pulmonary toxicity concerns for carbon nanotubes.⁹⁸ this is not the only study that highlights the structurally dependent toxicity of NPs. Another study found that minor alterations to fullerene structures change lethal dose by over seven orders of magnitude.⁹⁶ Furthermore, in carbon nanotubes, it was found that as degree of functionalization increases degree of cytotoxicity decreases.⁹⁷ Additionally much work is being done regarding how to functionalize carbon NPs to reduce pulmonary injury (specific functionalization and biomimetic architecture for instance).⁹⁴ All this suggests the possibility that fullerenes and other carbon NPs, while currently facing toxicological issues, may not face such problems in their use in the future.

Liposomes

Liposomes are the first nanomedicine system that has been successfully translated to clinical applications.⁸¹ As such liposomal drug formulations are rather common among nanomedicine systems among which there are liposomal systems for targeting ARDS/ALI. Included in these are formulations which modulate reactive oxygen species within the vascular epithelium.^{102,103} This targets a common pathogenic pathway for many dangerous pulmonary conditions. Liposomes have been engineered in the past to target this pathway through the delivery of superoxide dismutase (an antioxidant) in functionalized liposomes.¹⁰³ Antibody coated PEG liposomes loaded with EUK-134 were specifically used to target PECAM-1 in the

lungs delivered from the bloodstream. These liposomes inhibited cytokine induced inflammation in-vitro and accumulated in the lungs. Other liposomal formulations containing antioxidant enzymes have been used to mitigate the harmful effects of extracellular reactive oxygen species as well.^{104–106} Overall, liposomes are a highly effective nanomedicine system with a proven track record. It is a highly conventional system for the delivery of various payloads and can be easily functionalized.

Nano and Microemulsions

Emulsions of various types are a highly attractive drug delivery system. As with other nanomedicine systems, they enhance therapeutic efficacy of drugs and minimize adverse/toxic reactions.¹⁰⁷ Furthermore, they improve drug bioavailability^{108,109} among a host of other improvements as compared to the naked drug and are even easier to produce as compared to other Nanomedicine system. Furthermore, these structures can contain different and multiple phases within thereby solubilizing different substances including different gases. To tackle ARDS/ALI, this characteristic gives more options. Not only can antioxidants be delivered to deal with reactive oxygen species but also delivery of physiologically important gases.¹¹⁰ There are many methods by which emulsions can target ARDS/ALI and the following examples will cover that.

Among potential approaches to tackling ARDS/ALI, is emergency treatment to alleviate symptoms. Using dimethyl silicone is one such intervention and has been used in the treatment of early pulmonary edema associated with ALI.¹¹ Dimethyl silicone aerosols, however, utilize dichlorodifluoromethane as a major component. This compound is considered ecologically unsafe.^{11,111} Avoiding the issue of dichlorodifluoromethane, a novel class of emulsions has been used. Dry emulsions are lipid based powder formulations form which an o/w

nano/microemulsion can be reconstituted in-vitro or in-vivo.¹¹² Dry nano/microemulsions loaded with dimethyl silicone oil have been studied as an alternative.¹¹ The dry nano/microemulsion used as an inhalation can directly deliver dimethyl silicone to the lungs to exert its properties as a defoamer and alleviate symptoms of ARDS/ALI. Dry nano/microemulsions are a unique class of nano/microemulsions in that they can create a nano/microemulsion formulation that need not be aerosolized for delivery. This has unique advantages such as the removal of propellant from a typical direct to lung delivery mechanism as is the case with an inhaler.

More conventional classes of nano/microemulsion have been used in ARDS/ALI as in the cases where antioxidants or vital gases are delivered to the lungs. These modes of delivery are typically conducted intravenously. Perfluorocarbons (PFCs) do not interact and are separated from the carbohydrate reactions of biological chemistry. Furthermore, they can dissolve gases and do not themselves interact with the body.¹¹³ This makes PFC nanoemulsions extremely useful as gas carriers within the body. PFC nanoemulsions administered intravenously were shown to significantly alleviate ALI induced by LPS.¹¹⁰ PFC infusion was demonstrated to reduce neutrophil infiltration into lung tissue: a core pathogenesis of ALI/ARDS. PFC nanoemulsions can be made readily and PFC in of itself does not interact with the body. This makes them ideal candidates for the delivery of gases. Furthermore, they can be made into triphasic hydrocarbon oil-PFC nanoemulsions that can simultaneously deliver drugs as well.⁷⁹

PFC Nanoemulsions for Immune Cell Imaging

The key to using PFCs for *in vivo* imaging rest in the technology for fluorine NMR and by extension its use as a tracer agent in Fluorine MRI. This has all been mentioned in a prior section regarding the use of PFCs as an imaging agent. This section will primarily deal with PFC nanoemulsions as a formulation; how these formulations work, the rationale of their design, and

examples of PFC nanoemulsions in use. PFCs do not mix with cell membranes, in fact they are neither lipid nor water soluble.³⁰ In principle, they must be formulated into nanoemulsions, for which the ideal size of such a colloidal formulation is such that the droplet size is less than 200 nm.³⁰ A significant body of work exists for PFC nanoemulsions in the context of vascular imaging agents and as blood substitutes.^{114–116} In these applications nanoemulsions must be stable in vascular circulation for many hours. The surfactants used in these types of formulations should also provide passive or active targeting to macrophages.

With regards to how they behave, PFC nanoemulsions for imaging must meet similar criteria as nanosystems for drug delivery. There are certain criteria they must meet in order to target the intended cells.¹¹⁷ PFC nanoemulsion for imaging therefore must meet the criteria of targeting the cells relevant in inflammation while also delivering their payload. In this case the payload is PFC for imaging. Furthermore, the mode of delivery also plays a critical role in the design of the nanoemulsion. For *ex vivo* cellular delivery, PFC nanoemulsions should ideally follow these design criteria: droplet size less than 200 nm, low polydispersity index of less than 0.2, maximum fluorine to surfactant ratio in order to minimize the amount of MRI inactive material delivered to the cell, a surface that promotes cell membrane interaction, long term intracellular retention, a long shelf life, low toxicity, does not modify cell phenotype, and able to label a wide range of cells.³⁰ Large nanoemulsion droplets, for instance can affect cell activation phenotype after labelling.³¹ tight droplet size, indicated by the low PDI, helps ensure uniform labeling within the cell population.³¹

In addition to PFC structure, the choice of emulsifier is critical to the nanoemulsions ability to perform as an *in vivo* immune cell imaging agent. Stable emulsifiers for such an application must be non-toxic, chemically stable, help reduce the large interfacial tension of

PFCs in the aqueous phase,³⁰ and allow for cellular uptake by macrophages. Among all the possible emulsifiers phospholipids and Pluronics® are the most common.¹¹⁴ PFC nanoemulsions have been prepared using safflower oil and lecithin to stabilize PFOB base nanoemulsion.¹¹⁸ The resulting nanoemulsions had a droplet size of 224 nm with a PDI of 0.35. This PDI indicates a heterogeneous spread with regard to droplet size. In addition to traditional lipid based surfactants, there are Pluronics®. One of the earliest reported nanoemulsions, in fact, utilized Pluronic® F68 to generate a highly stable nanoemulsion.¹¹⁹ F68 stabilizes PFC oil droplets in aqueous phase mostly by steric effects.¹²⁰ Previous structural studies have shown that the block copolymer (F68) adsorb onto the interface between colloid PFC and the aqueous phase and that this adsorption is dependent on the electrolyte concentration in solution.^{121–123} This is to say that the stability of Pluronic® F68 based nanoemulsions can be tuned with the additional dimension of electrolytes in solution. It should be noted that Pluronic® is the trade name of triblock copolymer known as poloxamer. It is characterized by groups of PPO sandwiched between PEO.

Overall, the construction of a PFC nanoemulsion for imaging of immune cells during inflammation does not differ, fundamentally, from the construction of other nanomedicine systems for the treatment of ARDS. This is because they do the same thing at a fundamental level. They must identify and target specific cells while delivering their payload. In this case that payload is PFCs and the target is immune cells. Size and surface properties play a critical role in the development of these capabilities. These can be determined by the surfactant used in the construction of the nanoemulsions. We will go further into detail regarding the utility of size and surface properties in later sections specifically detailing how they are used.

Micelles

Micelles are nanosized colloidal dispersion prepared from amphiphilic molecules. This forms a hydrophobic core that acts as a reservoir for hydrophobic drugs while a hydrophilic shell stabilizes the core.¹²⁴ This class of nanomedicine system has been used previously in addressing the need for an ARDS/ALI treatment. On such approach utilized GLP-1 self-associated with PEGylated phospholipid micelles¹²⁵, while another utilized a multitargeted approach wherein phospholipid micelles inhibited TREM1, reactive oxygen species, and HSP90.¹²⁶ GLP-1 is an amphipathic hormone shown to hold promising immunomodulatory, anti-inflammatory, and anti-apoptotic effects. This particular drug formulation was administered via subcutaneous injection. It was found to suppress lung inflammation in LPS induced ALI in mice. This formulation is a successful example of the use of anti-inflammatory/antioxidant agents in nano systems targeted towards ARDS/ALI. An even more effective approach is to target multiple elements of ARDS/ALI pathogenesis such as in the second mentioned formulation. This formulation takes a combination of 3 drugs that inhibit three distinct intracellular pro-inflammatory signaling cascades activated in ALI in order to down regulate NF- κ B, a proinflammatory transduction factor in the lung. In order to do this micelles were constructed of distearoylphosphatidylethanolamine covalently bonded to PEG2000, GLP-1, and TREM-1 to form sterically stabilized micelles of 15 nm. In the hydrophobic core drug such 17-AAG was included.¹²⁶ This particular example shows a startling degree of complexity from micelles as a nanomedicine system. Composed of a hydrophobic core and amphiphiles. Each component of the micelle, from the core to the shell and it's payload is used as part of a three pronged approach to engage an anti-inflammatory response in the lungs.

Polymeric Nanoparticles

Polymeric NPs are nanoparticle structures that are composed of polymer such as PLA or PLGA. They can either incorporate drug throughout their matrix or encapsulate the drug. The advantage in using polymeric NPs is low toxicity, high biocompatibility, and biodegradability.¹²⁷ This makes them ideal for tackling a wide variety of disease states, including ARDS/ALI. It has been found that therapeutic delivery methods that target the lungs are far more effective than non-targeted approaches.¹²⁸ Polymeric NPs have been studied for alleviating ARDS associated with the application of bleomycin.^{129,130} Bleomycin has been found to upregulate EphA2¹³¹ leading to increased vascular permeability and inflammation.¹³⁰ In order to combat this side effect of bleomycin, a polymeric NP functionalized to downregulate EphA2 activation were developed. These NPs were functionalized with YSA peptide in order to downregulate EphA2 activation. This NP was delivered via tail vein injection.

Lipid Based Nanoparticles

The focus of this section will be on NLCs as opposed to SLNs. NLCs are considered an advanced and improved form of SLNs and examples of NLC should roughly apply to SLNs. An example wherein NLCs have been used to target ARDS/ALI is through the development of dexamethasone loaded NLCs.¹³² These NLCs utilize ICAM-1 antibodies conjugated to dexamethasone loaded NLCs to induce an anti-inflammatory response. Dexamethasone has previously been used to treat ALI patients and great interest remains in its use for its anti-inflammatory and anti-fibrotic characteristics.¹³³ This particular NLC was administered via tail vein injection. This NLC demonstrated enhanced lung targeting and superior reduction of inflammation.¹³²

Quantum Dots

Quantum dots are of particular interest for their optical and electrical properties. These properties make them ideal in imaging applications, however, they can also be utilized in drug delivery.¹³⁴ Actual application of quantum dots to pulmonary drug delivery in the lungs is of great interest to researchers for their diagnostic capacity in drug delivery.¹³⁴ There are some road blocks to large scale clinical applications, however. The vast majority of quantum dots, for instance are believed to induce cytotoxicity to some degree. This cytotoxicity, to a great extent depends on different factors that can be tuned based on the quantum dot.¹³⁵ In fact, there are new varieties of quantum dots designed to mitigate toxicity concerns such as carbon quantum dots and biomolecule derived quantum dots.¹³⁶ These biomolecule dots in particular have an inherent biocompatibility and a high degree of cellular uptake. While conventional, cadmium based, quantum dots may not find a high degree of applicability in ARDS/ALI, biomolecule derived “biodots” do. DNA under high pressure and temperature, condense to form these luminescent biodots.¹³⁷ Quantum dots conjugated with tumor specific ligands or antibodies or peptide were observed to be efficient for the detection and imaging of human tumor cells.¹³⁴ This bodes well for the principle of quantum dot drug delivery mechanisms as drugs have also been conjugated with quantum dots and are able to accurately target cancer cells.¹³⁸ while much work in quantum dots is focused on cancer research, there have been forays into targeting inflammation. Specifically, there has been work done to target chemotherapeutic agents to alveolar macrophages and inflammation.¹³⁹ This particular study found Quantum Dot conjugated doxorubicin enhances intracellular uptake as compared to free drug. Furthermore, uptake by

alveolar macrophages do not elicit a significant pro-inflammatory cytokine response. In-vivo this translated to uptake by alveolar macrophages without any evidence of ALI. Should this drug delivery system be translated to ARDS/ALI it could prove to be highly effective. Not only does it directly target inflammation, but the necessary drugs may be conjugated to the Quantum dot as necessary. This particular formulation was administered via inhalation.

Tuning of Nanomedicine for Pulmonary Applications

Nanomedicine Size

Particle size and size distribution is one of the most important characteristics of nanoparticles. Optimal size of NPs depend on the specific location and type of targeted tissues.¹⁴⁰ These factors determine in-vivo distribution, biological fate, toxicity, drug loading, drug release, stability and targeting ability of the system.¹⁴¹ Their small size, as compared to microparticles, such as higher intracellular uptake with nanoparticles 100 nm in size having 15-250 fold the uptake of microparticles. In fact, it has been found that nanoparticles are taken up by the majority of cell types while larger particles are not.¹⁴² It seems that particle distribution, can , in part, be tuned by controlling particle size.¹⁴¹ In systemic inflammation for instance, nanoparticle distribution is affected in a size dependent manner.¹⁴³ In particular, nanoparticles tend to aggregate within the lungs, liver and spleen regardless of size. This means that nanomedicine systems passively target the organ system of interest in cases of ARDS/ALI. Lungs specifically show, plentiful nanoparticle uptake, mainly outside of blood vessels.¹⁴³ This makes nanomedicine treatments all the more effective in ARDS/ALI. NPs within the nanometer size range are ideal for pulmonary targeting via intravenous delivery. Furthermore, there are many obstacles towards NP targeting of the lungs. Rapid bloodstream clearance by mononuclear phagocytes is one of the major obstacles.¹⁴⁴⁻¹⁴⁶ Modulation of pharmacokinetics of NPs to

prevent rapid clearance can be achieved by altering NP size.^{146,147} It must be noted that direct to lung delivery via inhalation is subject to different constraints than intravenous delivery. Particles of various size deposit in different regions of the lungs depending on particle size. It was found that 1-3 μ m particle deposit optimally within the alveolar region.⁶³

Cellular uptake in particular can be affected by variations in particle size. Various studies have tested particle size with different tissue types and found optimal NP sizes for those particular tissue types.¹⁴⁰ These studies show a clear trend in size dependent behavior on cellular uptake. There are distinct mechanisms influenced by the size that govern NP and cellular receptor adhesion.¹⁴⁸ An optimum NP size arises as a result of these mechanisms. As such, even though the lungs are already a prime target of submicron sized NPs, it is crucial to recognize which cells are being targeted in ARDS and tailor NP size to that cell/tissue type. For instance, the exudative phase of ARDS results in injury to both the capillary endothelium and the alveolar epithelium, with type I alveolar epithelial cells particularly susceptible to injury.¹⁴⁹ This makes the alveolar epithelium a target of particular interest for nanomedicine systems in ARDS/ALI. Previous *in vitro* and *in vivo* studies suggest that inhaled nanomaterials can penetrate epithelial cells for drug delivery.¹⁵⁰ In another study it was found that unmodified polystyrene NPs of size 50 nm were taken up by type I alveolar epithelial cells more effectively than similar particles of 100 nm in size.¹⁵¹ While this study does not find a particular optimum size it does demonstrate that the principle of size based targeting does hold for the alveolar epithelium and that smaller particles are better for targeting of the epithelium. When designing a nanomedicine system for ARDS/ALI size is a critical factor to account for. As for what particle size is best, it should be noted that most *in-vitro* studies show a maximum cellular uptake between 10 and 60 nm, regardless of core composition or surface charge.¹⁴⁰ Below 6 nm in diameter NPs are quickly

secreted by the body.¹⁴⁵ On the other hand, NPs larger than 200 nm aggregate in the spleen and liver, where they are processed by MPS cells.¹⁴⁴ Ideally this means that lung targeted NPs should range in size from 10 to 50 nm. In such fashion, there is the highest degree of uptake by cells and longer circulation times. Size selection is critical to the development of a drug delivery vehicle. While this section discusses size as it pertains to NPs, this does not preclude the data from being applicable to a variety of drug delivery vehicles and systems. Prudence must be taken in the selection of size and there is a large body of work to draw upon to inform the ideal size of the system.

Nanomedicine Shape

Shape is a critical property to the performance of NPs and a key part of NP design is determining the effects of variations in size, surface chemistry, and shape. NP shape is a critical factor to the performance of NPs. For instance, shape directly influences cellular uptake. Shapes showing the highest degree of uptake are rods followed, in order, by spheres, cylinders, and cubes.¹⁵² One will also have to consider the different potential orientations of the NPs and how they present themselves to cell surface receptors. It should be noted that while size and shape are different factors affecting NP behavior they also effect one another. For instance 50 nm is an ideal size for maximized cellular uptake by gold NPs, silica NPs, and single walled carbon nanotubes.^{107 153-155} The shape of NPs will also effect circulation time in the body, with rod shaped micelles having a circulation time ten times longer than their spherical counterparts. As a result of all these factors, shape selection is critical to the development of an effective ARDS/ALI lung targeted nanomedicine system. Sometimes there are no options when selecting the shape of the and by default the shape of the drug delivery vehicle. Some nanosystems by default create drug vehicles that are spheroid in nature, however, where there is choice the most

optimum choice must be made. Rods may be an ideal shape for some applications but perhaps increased cellular uptake and longer circulation times are not ideal. It is possible to tune these properties of a rod shaped nano-object by changing the long to short axis ratios. This will tune the properties that can be modified through a change of shape.

Surface Properties

The surface chemistry of the vehicle for targeted drug delivery is one of the most diverse and highly tunable aspects of a nanosystem for drug delivery. NP surface chemistry seems to determine the type of proteins adsorbed onto the surface and strength of that interaction.¹⁵⁶ As a result of the different proteins adsorbed onto the NP surface, the NP can take on a variety of different properties. Not the least of which, is the targeting that nanomedicine systems are designed for. In previous examples discussed, a variety of methods to functionalize NPs and drug delivery systems were presented. Among these systems, PEGylation, for instance, is a classic method to enhance circulation time of liposomes. This creates “stealth liposome” systems⁸² in which liposomes evade immune detection and are not consumed thereby circulating in the body for longer periods of time than conventional liposomes.¹⁵⁷ Surface charge must also be considered when designing a drug delivery system. Positively charged NPs are taken up at a much faster rate as compared to those with neutral or negative charges.¹⁴⁴ This is perhaps driven by electrostatic interactions between the NP and the cell membrane (negatively charged). This must, however, be balanced with the fact that positively charged NPs are also cleared most quickly from the blood and can cause certain complications.¹⁵⁸ There are many ways to modify the surface properties of nanomedicine systems aside from PEGylation and surface charge. For instance, drug can be bound to the surface of NPs to allow for rapid release of drug upon intake.¹⁵⁹ Sufficed to say, there are numerous methods to modify the characteristics of the

surface of nanosystems for drug delivery. Far too many methods exist, with new methods being generated every day. Fundamentally, surface property modification revolves around the addition of useful elements, be it charge, polymer chains, ligands, antibodies, etc., to modify a key parameter of the system. This is where the greatest degree of innovation and creativity can be exerted to optimize a nanosystem for pulmonary drug delivery for ARDS/ALI.

Metanalysis of Reported Nanoemulsions using Machine Learning.

The basis for this work rests on prior work by the Janjic lab in the realm of multiple linear regression (MLR) for predicting droplet size of complex PFC nanoemulsions.¹⁶⁰ In this prior work, MLR is presented as a novel methodological advancement for the development and optimization of perfluorocarbon nanoemulsions. It differs greatly from the work introduced here in that not only does it use a different method, but that it also uses an entirely different kind of data set. The data set used was derived from a series of formulations that make use of D-optimal mixture design to generate a curated collection of nanoemulsion formulations. These formulations isolated mixture variables and allowed for their study utilizing MLR. The data set generated for this application is therefore a highly homogeneous data set with similar nanoemulsions that differ only by variation of certain factors. The data set utilized in this machine learning application, on the other hand, is highly heterogeneous with nanoemulsion data gathered from a variety of differing sources. This is where the difference between the current work and the prior work comes into play. Machine learning is a process by which machine learning algorithms are applied to large amounts of data and patterns extracted from that data. MLR similarly has the capacity to extract patterns from the data to create a statistical model of the data. However, these two means of learning differ. MLR is a form of multivariate statistical

analysis, these methods underpin much of the framework of machine learning. In a sense, this is to say that MLR is a single method whereas machine learning is a collection of methods.

Machine learning is more nuanced application of statistical methods such that the model may “learn” the effective solution for the set of data being worked with. MLR on the other hand is a statistical method generates a model that allows for the understanding of the relationship among the data collected. In short machine learning is a high level technique that employs multiple statistical methods to make sense of data whereas MLR is a single statistical method.

Introduction to Machine Learning

The digitization of industrial processes has generated a great deal of data regarding these processes and the products of those processes. In order to optimizes such processes to save time, resources, and avoid general waste, machine learning and artificial intelligence has been applied to them.¹⁶¹ As with any manufacturing process, this can be applied to the manufacture of perfluorinated nanoemulsions. Machine learning has not in the past been applied to the manufacturing process of perfluorinated nanoemulsions. Machine learning is useful in cases such as where traditional optimization methods have reached their limits.¹⁶² In situations wherein the relevant data is not reported holistically, this is especially critical.

At the heart of this research is the use of bootstrap aggregation (bagging). Bagging includes the creation of multiple copies of the original training data and using the bootstrap, fitting a separate decision tree to each copy, and then combining all the trees. Bagging aims to create a single predictive model from these independently formed decision trees in order to reduce the problem of overfitting.¹⁶³ We use bagging to analyze the data set of processing and material parameters generated from the information found in the literature.^{79,164–189}

Bagging has never been used to analyze the manufacturing process of perfluorinated nanoemulsions prior to this, however, it has found use in analyzing a variety of other manufacturing procedures.¹⁹⁰⁻¹⁹² In the domain of heavy process manufacturing, for instance, there is a wealth of historical data that can be analyzed and has been analyzed using bagging.¹⁹⁰ The ensemble nature of bagging as a model makes it impossible to understand the precise relationship between input and output variables, however, it is possible to quantify impact of predictors in the ensemble.¹⁹³ It possible to understand the extent to which certain inputs affect the outputs.¹⁹¹ All this being said, machine learning and bagging in particular is an excellent method with which to analyze data for any manufacturing process this includes the manufacture of perfluorocarbon nanoemulsions.

Colloidal Properties of Nanoemulsions and Machine Learning

Before understanding the application of machine learning to colloidal properties of nanoemulsions, colloidal properties must first be contextualized. Size refers to the diameter of nanoemulsions droplets. Zeta potential refers to the electrical potential of the plane of the interface which separates the mobile fluid phase from the fluid phase that remains attached to the surface of the nanoemulsion droplet. Zeta potential therefore can be considered a type of surface potential. PDI on the other hand refers to poly dispersity index and indicates the heterogeneity of the sizes of a colloidal sample.

Zeta potential is a measure of surface potential of colloidal particles when placed in liquid. Zeta potential is used for predicting dispersion stability and its value depends on physiochemical properties of drug, vehicle, presence of electrolytes, and their adsorption.¹⁹⁴ however, not only is zeta potential important for the stability of nanoemulsions but they are also important for targeted delivery and cellular uptake.¹⁹⁵ With regard to targeted delivery, this comes as no

surprise as it was previously indicated that surface properties are critical to targeted drug delivery. In order to measure zeta potential, an electric field must be applied across the dispersion. Particles move towards the electrode of opposite charge with a speed proportional to the magnitude of the zeta potential.¹⁹⁵

Size is another important nanoemulsion colloidal property. As discussed in a previous section, the passive targeting of nanomedicine systems depends greatly on the size of the nanomedicine system. For nanoemulsions, however, size is intimately related to PDI. Size is measured using dynamic light scattering (DLS). This is a technique wherein light scattered is used to detect the Brownian motion of particles and this is correlated to size and size distribution of said particles.¹⁹⁴ Finding size distribution allows one to find PDI as well. PDI may take on any value between zero and one where a PDI of zero indicates a monodisperse system and a PDI of one is a polydisperse system.¹⁹⁶

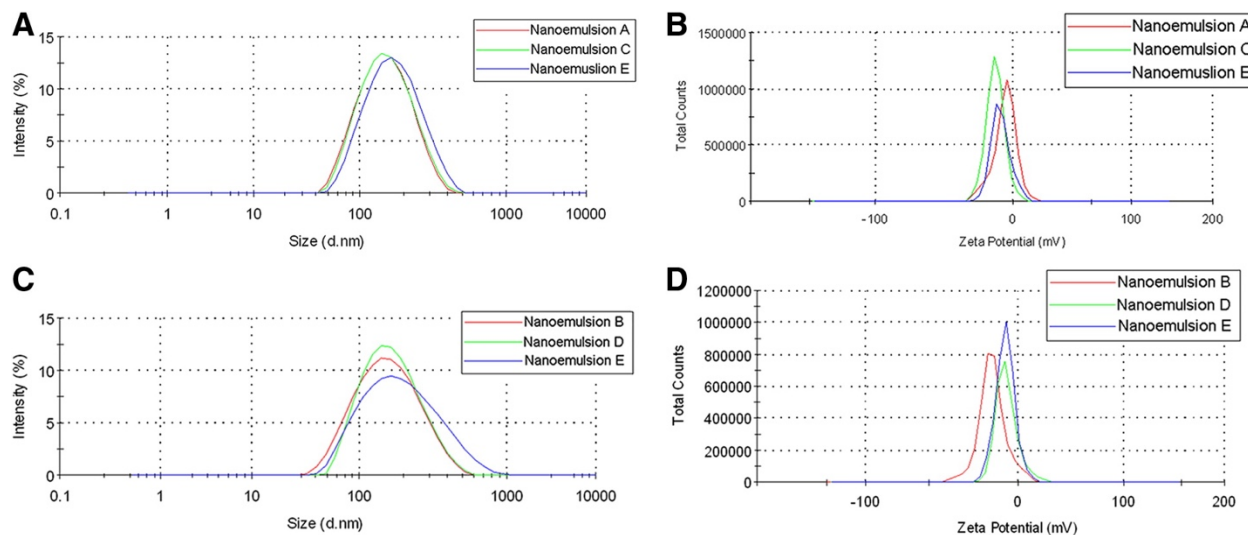


Figure 1. Representative examples for size and zeta potential distributions for small(nanoemulsions A and B), medium (C and D), and large (E and F) scale nanoemulsions. Definitive size and zeta potential measurements are actually averages of those distributions.

Figure reproduced from Ref.¹⁶⁶

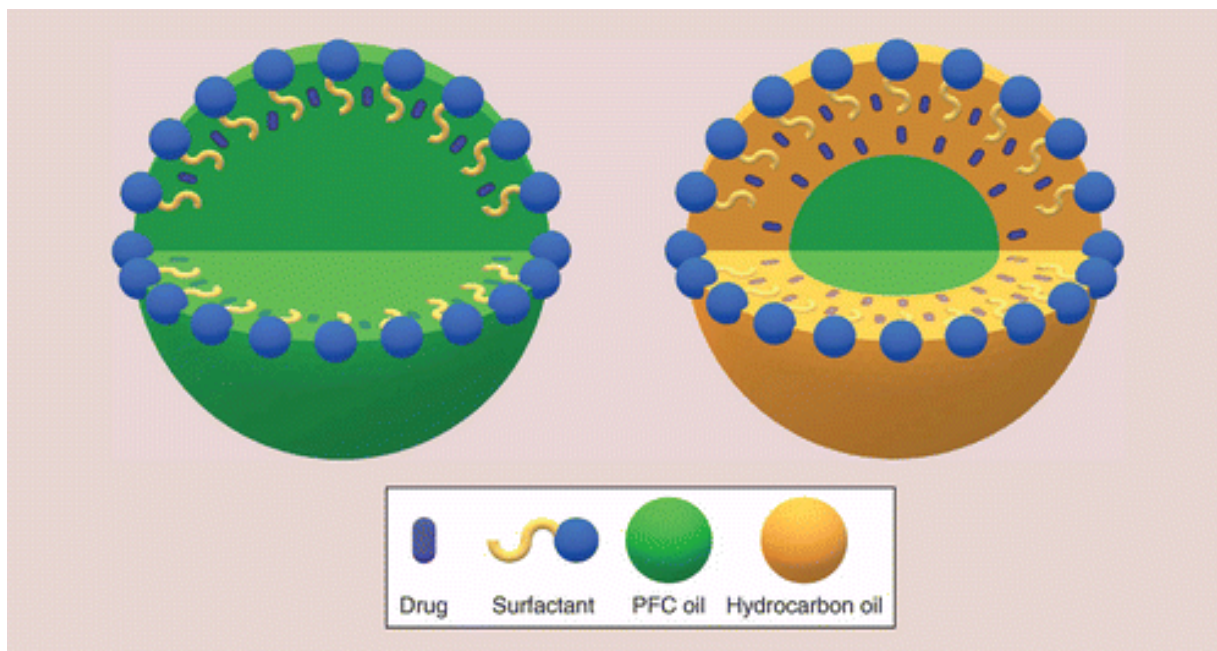


Figure 2. Schematc representation of structural differences between traditional biphasic (left) nanoemulsions and triphasic (right) nanoemulsions. Both these nanoemulsion types are included in the machine learning analysis. Image reproduced from Ref.⁷⁸

Moreover, there must be a discussion regarding the types of nanoemulsions being analyzed during the machine learning analysis portion of this paper. Both biphasic and complex nanoemulsion formulations are fed to the machine learning algorithm. These nanoemulsions have a significant degree of difference from one another. Complex nanoemulsions have two layers and utilize hydrocarbon oils in addition to PFC oils. This makes them much more complex and modeling them alongside biphasic nanoemulsions is an additional challenge to the model. They should be modeled, however, as multiple phase nanoemulsions have broader utility as compared to simple biphasic nanoemulsions.¹⁹⁷ One should refer to figure 2 to distinguish between these complex and biphasic nanoemulsions. Biphasic nanoemulsions are characterized

by a single phase within the nanoemulsion whereas the complex nanoemulsion is characterized by multiple phases.

Methods

The methods discussed in the following section will cover the following: how and what data was gathered and why, how this data was prepared for machine learning analysis, the machine learning analysis itself, analysis of the generated data, and predictions utilizing the model. These five steps cover the, essentially, what was done in the course of the machine learning analysis of the data. We will cover topics such the algorithm used in the machine learning analysis, how the data was analyze using MATLAB, and the results of the various analysis.

Data Collection Process

The data collection process focused on obtaining complete formulation data from a variety of peer reviewed journals and patents. As this data is intended for a machine learning analysis, dependent and independent variables must be identified and parsed. With regard to dependent variables, it was proposed that a thorough understanding of composition and process parameters are necessary for quality microemulsion development.¹⁹⁸ While not nanoemulsions, microemulsions are a closely related nanomedicine system. Therefore, we viewed these compositional and processing parameters with critical importance as independent variables. These parameters included PFC concentration, PFC type, solvent type, solvent concentration, exposure to microfluidization, degree of said exposure, and many other variables pertaining to the composition and the forces to which the nanoemulsion formulation was exposed to.

With regard to dependent variables, we considered these to be critical quality attributes (CQAs) identified by the Janjic lab in previous works.¹⁹⁸ These CQAs included size and PDI. In addition to size and PDI, we included surface zeta potential as parti of the dependent variables as

well. Dependent variables are what we will be looking towards to judge the efficacy of the generated model. Through the ability of the model to predict these dependent variables we will judge the effectiveness of the method employed. As such these dependent variables are critical to model development.

Data Preparation Process

Raw unprocessed data, such as nanoemulsion formulations and processing, are not amenable to machine learning analysis inherently. It must first be broken down into a list of static features that can be automatically processed by the algorithms. In order to do this material lists were broken down into their broader components and the processing lists broken down into their specific characteristics.

Blends of PFCs, surfactants, excipients, active drugs, and buffers were broken down into their components and listed separately. As concentrations can be reported in three different ways (w/w%, v/v%, and w/v%) these categories were reported as well. This was done for ease of data processing as well as giving the model exposure to more data. Processes, such as microfluidization, was broken down into component information such as microfluidization PSI and number of passes. This resulted in features that could roughly be broken down into approximately 28 broad categories encompassing 57 different features (dependent and independent variables). While this may seem like a lot of features, especially for the given amount of information, many of these features were highly related to one another. As a result of this there were some features for some nanoemulsion formulations that could not be filled out as it simply did not exist. Data that did not exist or was uncertain were treated similarly and indicated in the data prepared for the model. This is not to say the missing or uncertain data was

ignored. Rather this data was indicated as uncertain using the “NaN” variable in MATLAB®. This implies that the value is unknown.

Machine Learning Analysis

In order to analyze the data through machine learning algorithms, MATLAB was employed. More specifically, the regression learner applet was used to apply bootstrap aggregation to the data to generate a model of the data. Bootstrap aggregation, also known as bagging, is a process by which data is separated into various partitions with replacement and individual decision tree models fitted to each bootstrap. These decision tree models are then aggregated into a single model. This makes for a more robust model that avoids the problem of overfitting the data.

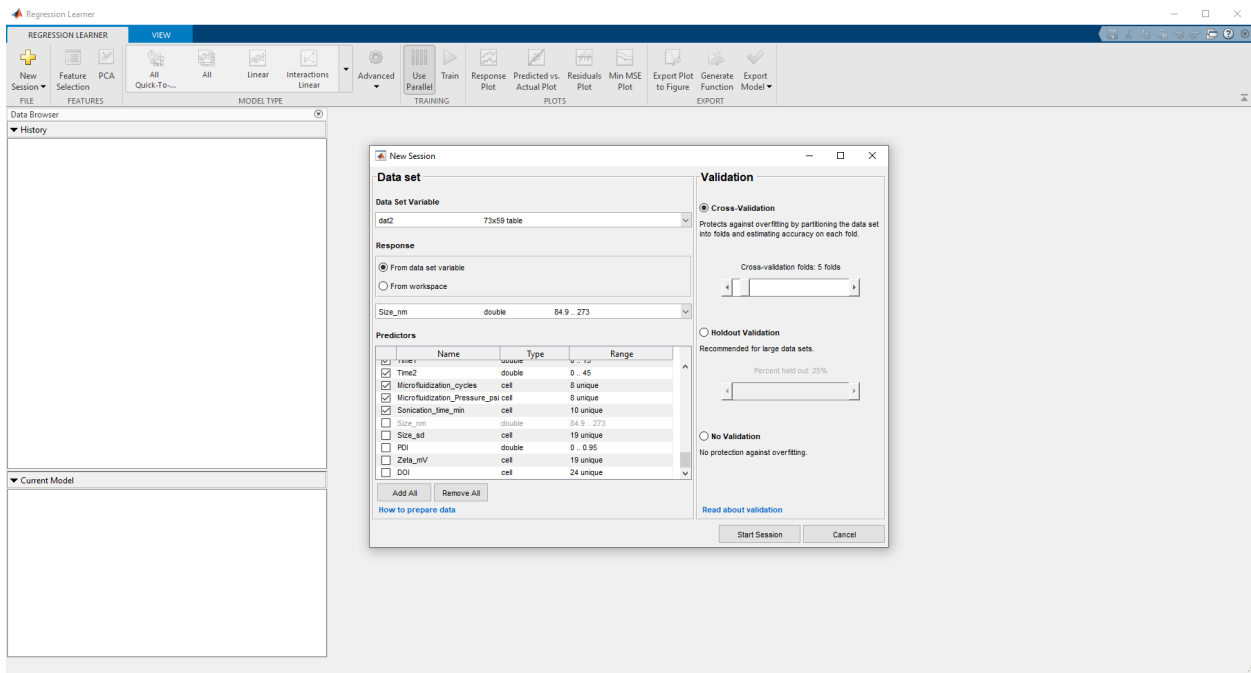


Figure 3. Internal image of the setting up of the regression learner applet. Here size is the designated dependent variable of the machine learning algorithm.

In setting up the model, it should be noted that the data is internally validated utilizing a cross-validation method. In this method, the data is partitioned into a number of folds (or divisions). For each fold, a model is trained using out of fold observations and then model performance is assessed using in fold data. The averages are calculated across all folds to give the average error. This means of internal validation was automatically used to ensure that overfitting did not take place. In figure 3, this is indicated on the sliding bar in the upper right corner. The data set used is partitioned into five folds in this case and trained in such a manner. Overfitting is a problem wherein the model generated by the algorithm is too specific to the training data set and cannot be effectively generalized to other data. There are approximately 15 data points to each fold. The MATLAB® applet does not allow one to choose these data points manually however it is possible to create a composite model wherein one has greater control over this process. Done later in through the process of internal validation and yields results similar to the ones derived directly from the model. More detail will be given in the section regarding predicitions/validation.

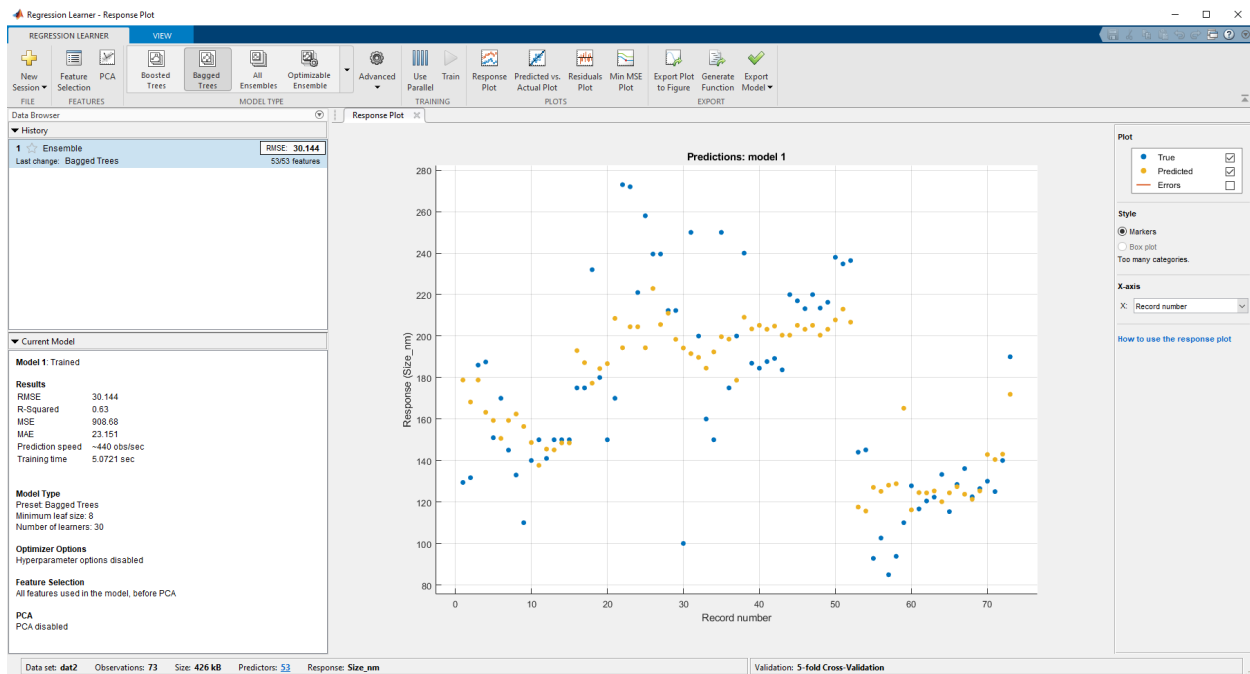


Figure 4. An example model generated from the data gathered. It has an RMSE of 30.144 and an R^2 value of 0.63.

Figure 4 is an example model generated by the machine learning algorithm employed; more specifically, it employs the bootstrap aggregation to generate the model. Furthermore, not just bagging was used to generate a model. Eighteen other machine learning algorithms were employed. These eighteen algorithms were eventually discarded from use for a variety of reasons. Three failed to produce a model outright for various reasons, nine overfit the data, two were similar to taking averages of the data, and three failed to respond to variation of the input stimuli. Of the two remaining algorithms left (bagging and boosting), bagging was ultimately chosen for its ability to avoid the problem of overfitting the data. The nineteen models have been included in the supplementary tables and figures section.

Analysis of Model and Generated Data

In order to analyze the model and how each input variable affected the output model generated, the inputs were varied, and the outputs recorded. This variation of inputs testing allowed for assessment of the relative importance of different variables by assessing the impact that removal of dependent variables would have on the RMSE and R^2 values. As a result, it is possible to determine the relative importance of the variables to the overall fit of the model but not how, more specifically, they impact the model. This is no real issue and does not result in any loss of data as ensemble of tree methods inherently do not allow for one to determine how variables impact the model. Only their relative importance is a factor that can be known.

Predictions and Validation

Results of the model were used to predict two different data sets and these two data sets were used to validate the predictive capabilities of the model in different ways. One data set utilized the existing data already used to generate the primary predictive model to validate the method of generating the predictive model. This method will be termed here as internal validation. The other method by which the model was validated was to use the model to predict data from outside of the original data set. This method will be termed external validation. Both the internal and external validation methods are designed to detect the problem of overfitting. Internal validation detects the problem of overfitting by assessing the goodness of the algorithm itself for generating a model while the external validation method assesses the effectiveness of the model itself. This means that internal validation looks towards the data the model uses and manually validates the model in a manner similar to Both these methods, together, should detect the problem of overfitting and allow one to assess how good the model is with regards to making

actual predictions. As the goal of this model is to eventually be used to predict colloidal properties of nanoemulsions, this is critical.

Results

Results can be broadly broken down into three broad categories: the models generated, the results from the validation (external and internal), and data generated through model exploration. The results from these three categories will respectively describe how efficacious machine learning is at generating a model that fits the data, whether this model is valid as a means of predicting data outside of the model, and what features are important to the accuracy of the model and therefore may be good predictors for those colloidal properties.

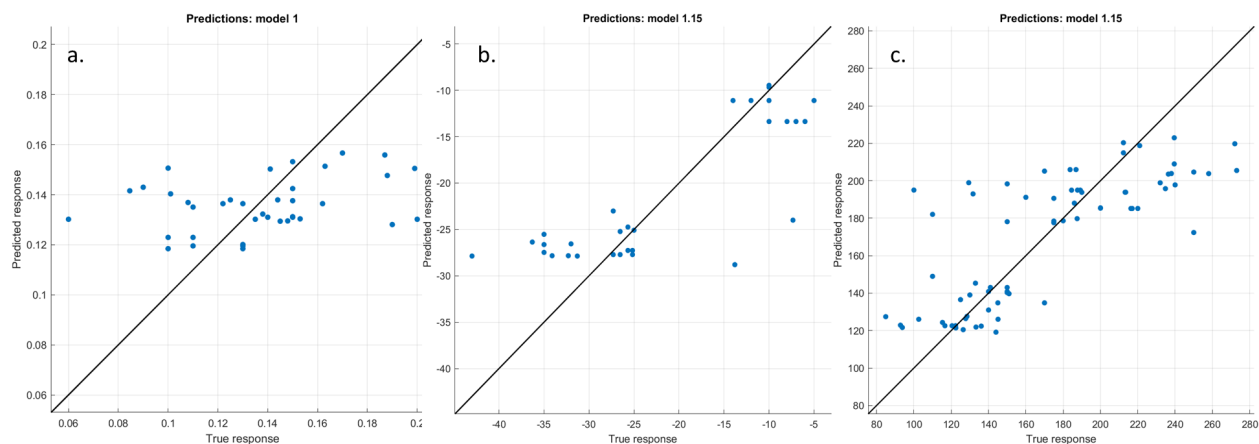


Figure 5. Response plots of PDI, zeta potential, and size (left to right). These models have respective R^2 values of 0.14, 0.69, and 0.58. These response plots correspond to the training data sets. The predicted values are in yellow whereas the actual values are in blue.

Figure 3 contains the model data for the training data used to construct those models. On these response plots, the x-axis corresponds to the entry number as opposed to any dimension of the data's features. The y-axis on the other hand corresponds to the independent variable that is being measured. For the PDI this is unitless, whereas for zeta potential this is in mV while size is in nanometers. These values indicate that the model was capable of generating predictions for both size and zeta potential but not able to accurately make predictions for PDI. A value close to zero for R^2 indicates that the model is only slightly better than taking an average of the data and using that as a prediction. This can be seen in how the data in the response plot for PDI clusters about a central line for the most part. These R^2 values indicate the predictability of the data and as such they indicate that the zeta potential and size are relatively predictable based on the information given whereas PDI is unpredictable for the most part.

Table 1. These values are the results of the variation of inputs study on the size model. Baseline is indicated on the first row with no features removed. Following entries to the table indicated various features being removed.

| Model | RMSE | R-square | MSE | MAE | Feature Removed 1 | Feature Removed 2 | Feature Removed 3 | Feature Removed 4 | # of Features Removed |
|-------|--------|----------|--------|--------|-------------------|-------------------|---------------------|-------------------|-----------------------|
| 1 | 31.103 | 0.58 | 967.39 | 22.958 | NA | NA | NA | NA | 0 |
| 2 | 31.517 | 0.57 | 993.31 | 23.817 | PFC type | NA | NA | NA | 2 |
| 3 | 30.865 | 0.59 | 952.67 | 23.359 | NA | PFC conc | NA | NA | 5 |
| 4 | 34.526 | 0.49 | 1192.1 | 25.94 | PFC type | PFC conc | NA | NA | 7 |
| 5 | 35.013 | 0.47 | 1225.9 | 25.818 | Surfactant type | NA | NA | NA | 3 |
| 6 | 31.764 | 0.57 | 1008.9 | 23.79 | NA | NA | Surfactant Category | NA | 3 |
| 7 | 33.493 | 0.52 | 1121.8 | 24.836 | NA | Surfactant conc | NA | NA | 7 |
| 8 | 35.106 | 0.47 | 1232.4 | 27.304 | Surfactant type | Surfactant conc | Surfactant Category | NA | 13 |
| 9 | 31.535 | 0.57 | 994.47 | 23.964 | Buffer type | NA | NA | NA | 1 |
| 10 | 35.752 | 0.45 | 1278.2 | 26.139 | NA | Buffer conc | NA | NA | 2 |
| 11 | 31.299 | 0.58 | 979.64 | 23.202 | NA | NA | Buffer pH | NA | 1 |
| 12 | 34.421 | 0.49 | 1184.8 | 25.473 | Buffer type | Buffer conc | Buffer pH | NA | 4 |
| 13 | 31.69 | 0.57 | 1004.3 | 23.906 | Active Drug | NA | NA | NA | 1 |
| 14 | 31.547 | 0.57 | 995.21 | 23.727 | NA | Active Drug conc | NA | NA | 1 |
| 15 | 35.345 | 0.46 | 1249.3 | 26.476 | Active Drug | Active Drug conc | NA | NA | 2 |
| 16 | 31.198 | 0.58 | 973.3 | 23.553 | Solvent type | NA | NA | NA | 1 |
| 17 | 35.233 | 0.47 | 1241.3 | 25.839 | NA | Solvent conc | NA | NA | 2 |
| 18 | 30.694 | 0.6 | 942.09 | 23.252 | Solvent type | Solvent conc | NA | NA | 3 |
| 19 | 35.35 | 0.46 | 1249.6 | 26.315 | Excipient Type | NA | NA | NA | 4 |
| 20 | 32.453 | 0.55 | 1053.2 | 24.21 | NA | Excipient conc | NA | NA | 7 |
| 21 | 35.024 | 0.47 | 1226.7 | 26.747 | Excipient Type | Excipient conc | NA | NA | 11 |
| 22 | 34.079 | 0.5 | 1161.4 | 23.349 | NA | NA | RPM | NA | 2 |
| 23 | 33.744 | 0.51 | 1138.7 | 25.067 | NA | NA | NA | Time | 2 |
| 24 | 33.701 | 0.51 | 1135.8 | 24.999 | NA | NA | RPM | Time | 4 |
| 25 | 31.713 | 0.57 | 1005.7 | 23.953 | NA | NA | Micro Cycles | NA | 1 |
| 26 | 31.221 | 0.58 | 974.77 | 23.316 | NA | NA | NA | Micro PSI | 1 |
| 27 | 33.609 | 0.51 | 1129.5 | 25.556 | NA | NA | Micro Cycles | Micro PSI | 2 |
| 28 | 31.133 | 0.58 | 969.28 | 23.102 | NA | NA | Sonication | NA | 1 |

Table 2. These values are the results of the variation of inputs study on the zeta potential model.

Baseline is indicated on the first row with no features removed. Following entries to the table indicated various features being removed.

| Model | RMSE | R-square | MSE | MAE | Feature Removed 1 | Feature Removed 2 | Feature Removed 3 | Feature Removed 4 | # of Features Removed |
|-------|---------|----------|--------|--------|-------------------|-------------------|-------------------|-------------------|-----------------------|
| 1 | 6.3763 | 0.69 | 40.657 | 4.6322 | Baseline | NA | NA | NA | 0 |
| 2 | 6.3143 | 0.69 | 39.87 | 4.5345 | PFC Type | NA | NA | NA | 2 |
| 3 | 7.9434 | 0.51 | 63.097 | 5.0893 | PFC conc | NA | NA | NA | 5 |
| 5 | 7.4598 | 0.57 | 55.649 | 6.0169 | PFC Type | PFC conc | NA | NA | 7 |
| 6 | 7.0813 | 0.61 | 50.144 | 4.7278 | Surf Type | NA | NA | NA | 3 |
| 7 | 7.0847 | 0.61 | 50.193 | 4.6638 | Surf Category | NA | NA | NA | 3 |
| 8 | 7.324 | 0.59 | 53.641 | 5.115 | Surf Conc | NA | NA | NA | 4 |
| 9 | 8.3625 | 0.46 | 69.931 | 5.7156 | Surf Type | Surf Category | Surf conc | NA | 10 |
| 10 | 6.6463 | 0.66 | 44.173 | 4.9141 | Buffer type | NA | NA | NA | 1 |
| 11 | 7.5625 | 0.56 | 57.192 | 5.2897 | Buffer conc | NA | NA | NA | 2 |
| 12 | 60.0145 | 0.72 | 36.174 | 4.1317 | Bueffer pH | NA | NA | NA | 1 |
| 13 | 7.3944 | 0.58 | 54.678 | 5.0708 | Buffer type | Buffer conc | Buffer pH | NA | 4 |
| 14 | 6.2601 | 0.7 | 39.188 | 4.5542 | Active Drug | NA | NA | NA | 1 |
| 15 | 6.1523 | 0.71 | 37.851 | 4.4029 | Active drug conc | NA | NA | NA | 1 |
| 16 | 7.7162 | 0.54 | 59.54 | 5.5498 | Active Drug | Active Drug conc | NA | NA | 2 |
| 17 | 6.2475 | 0.7 | 39.031 | 4.6214 | Solvent Type | NA | NA | NA | 1 |
| 18 | 7.4741 | 0.57 | 55.862 | 5.3775 | Solvent conc | NA | NA | NA | 2 |
| 19 | 7.3071 | 0.59 | 53.394 | 4.9248 | Solvent Type | Solvent conc | NA | NA | 3 |
| 20 | 6.4205 | 0.68 | 41.222 | 4.5997 | Excipient Type | NA | NA | NA | 4 |
| 21 | 6.5202 | 0.67 | 42.513 | 4.839 | Excipient conc | NA | NA | NA | 4 |
| 22 | 7.616 | 0.55 | 58.003 | 5.4299 | Excipient Type | Excipient conc | NA | NA | 8 |
| 23 | 7.5918 | 0.56 | 57.635 | 5.3547 | RPM | NA | NA | NA | 2 |
| 24 | 7.8322 | 0.53 | 61.343 | 5.5507 | Time RPM | NA | NA | NA | 2 |
| 25 | 6.2642 | 0.7 | 39.24 | 4.6277 | RPM | Time RPM | NA | NA | 4 |
| 26 | 6.7696 | 0.65 | 45.827 | 4.9598 | Micro Cycles | NA | NA | NA | 1 |
| 27 | 6.7103 | 0.65 | 45.038 | 4.8571 | micro PSI | NA | NA | NA | 1 |
| 28 | 7.8083 | 0.53 | 60.97 | 5.6932 | Micro Cycles | Micro PSI | NA | NA | 2 |
| 29 | 6.6294 | 0.66 | 43.95 | 4.7779 | Sonication Time | NA | NA | NA | 1 |

Variation of input testing reveals other information through the variation in R^2 value.

Features are removed in batches of related features as removing the features individually would tell nothing regarding the actual importance of that data. Only when removed in these related batches is it possible to tell what data is actually important to the model. With regard to zeta potential, it can be seen in table 2 that surfactant type, category, and concentration play a large role in being able to make an accurate prediction. This can be seen by the large drop in R^2 value for each category of data and an even large cumulative drop when all three categories of data are removed. There are other factors as well that are important to zeta potential, though less so. These include categories of data for which an R^2 less than 0.55 results from their removal. With regard to size data a very different picture is painted. As can be seen from table 1, there is a much larger variety of factors that seem to play a role in size prediction and by extension what factors may play a role in determining the size of PFC nanoemulsions. There were some results, however that coincided with the results of previous work, wherein it was found that PFC oil type and concentration were critical to determining nanoemulsion size.¹⁶⁰



Figure 6. Data generated through the self-validation of the model. This composite model has an RMSE of 22.37 nm and an R^2 value of 0.639.

Going beyond simply exploring the model, the model was utilized to make predictions of size data. The reason only size data was used was because of size and zeta potential, only data for size was found for external validation. For this reason, only the size data was validated. It was found through the internal validation method, as shown in figure 4, that the model does not have the problem of overfitting. Since the composite model generated from utilizing the bagged tree method generated a model with an RMSE as low as 22.37 nm and a relatively high R^2 value,

it can be said that internal validation indicates, the model generated can be applicable to data outside the model. However these results contrast with those of the external validation testing shown in figure 4. Here the R^2 value is negative, therefore indicating that the model is not a good fit for the data. A low R^2 value (close to zero) implies that the prediction is no better than selecting the mean of the data. A negative R^2 value suggests that the fit of the data is worse than that. It implies that the predicted data do not follow the pattern of the actual data. In spite of this, the RMSE value is exceptionally low and indicates the model may not be entirely bad at predicting the size data. The predicted data^{78,199} however consists heavily of complex triphasic PFC nanoemulsions. The bulk of the data used to generate the models consisted of biphasic nanoemulsions. This difference may account for the relative degree of inaccuracy present in the model via external validation.

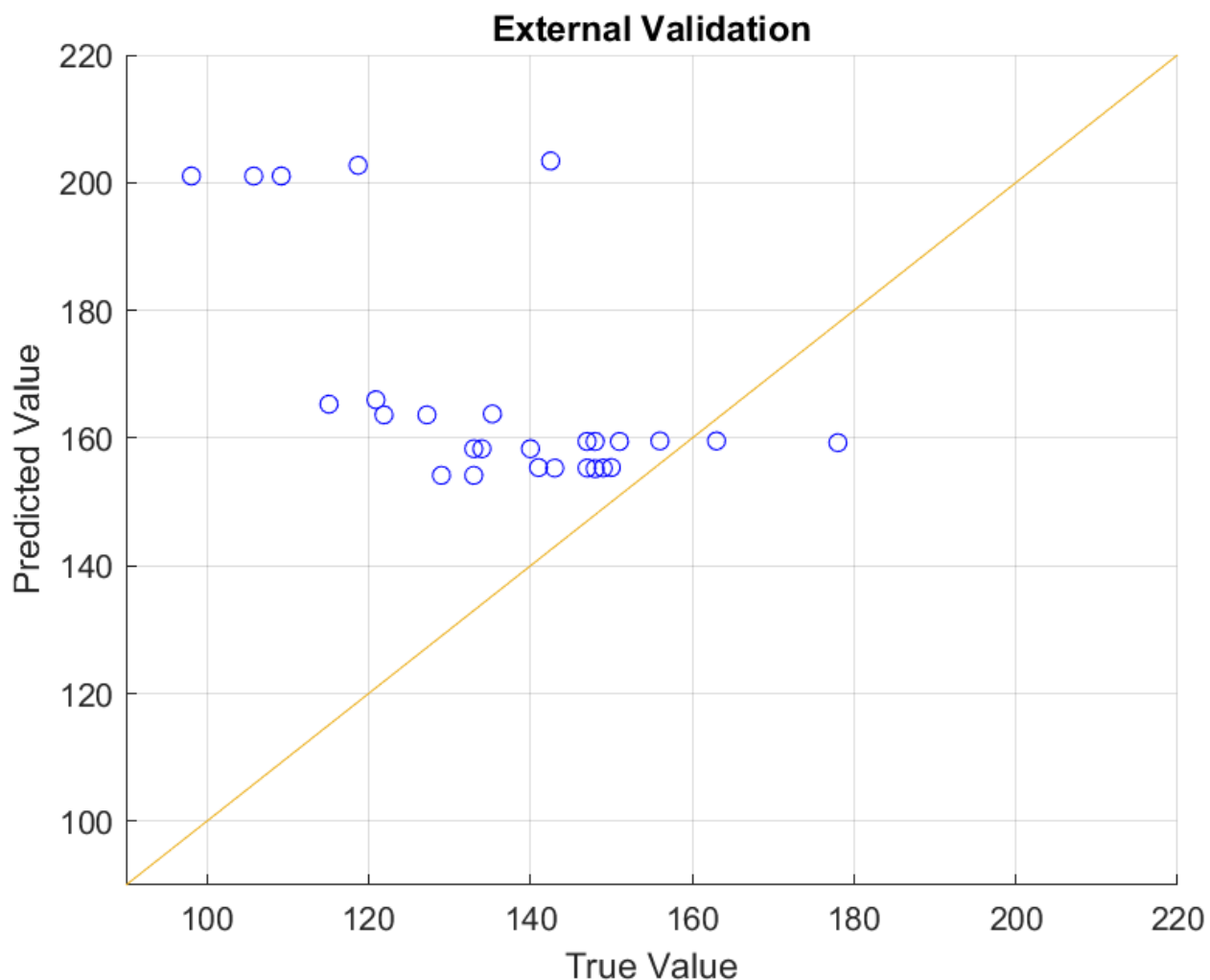


Figure 7. The external validation model with an RMSE of 20.45 and an R² value of -0.478.

Conclusion

Conclusions that can be drawn from the machine learning analysis are mixed with regard to the general utility of the model generated. While the initial models generated to predict size and zeta potential show good promise in being able to predict the data from the predictor data set, it is not enough to show the utility of the model. This is why validation is so critically important to the ensuring the model has good predictive capabilities outside of the training data set. To this end validation was employed, however the results of validation were mixed. Self-validating

utilizing the data from the training data set indicate that the model is just as good, if not better, at predicting data from outside of the data used to generate the predictive model. On the other hand, predicting data from completely outside the training data set indicates that model is not good at predicting size. This could be a result of not having enough data in the original training data set that would apply to the data from outside the testing data set. This is the most likely case, as there was a vast number of biphasic PFC nanoemulsion formulations used to train the data while there were only a few triphasic formulations to train the data set. As the testing set consisted primarily of triphasic, this can be where the failure derived from. In order to more effectively predict the data, more triphasic formulation data must be employed to train the model. In this fashion not only will the model be able to predict the size of biphasic nanoemulsions but also more complex triphasic nanoemulsions.

Overall results can be said to be mixed with regard to the results of using machine learning to assess predict the colloidal properties of PFC nanoemulsions. Size and zeta potential were found to be able to be predicted by the machine learning model to a certain extent, while PDI was impossible to predict. Regarding size and zeta potential, there were models that could be generated with relatively high R^2 values. With regard to validation, however, there mixed results regarding size. Internal validation indicated that size predictions using machine learning is a valid approach whereas external validation indicated that machine learning may not be the most optimal method by which to predict size. However, these mixed results may be the result of not having enough data to train the model. Results from external validation tended to cluster depending on the article form which data was derived. This, combined with the relative lack of complex triphasic nanoemulsions used to train the model, indicate that there was simply not enough breadth of data used to train the machine learning model. Before, this model can be

broadly applied to understanding the properties critical to the performance of PFC nanoemulsion nanomedicine systems, the training data set must be expanded. This thesis however provide a framework for using machine learning as a predictive tool once those necessary experimental measurements can be made.

Appendix

Supplementary Figures and Tables

Predictions: model 1.1

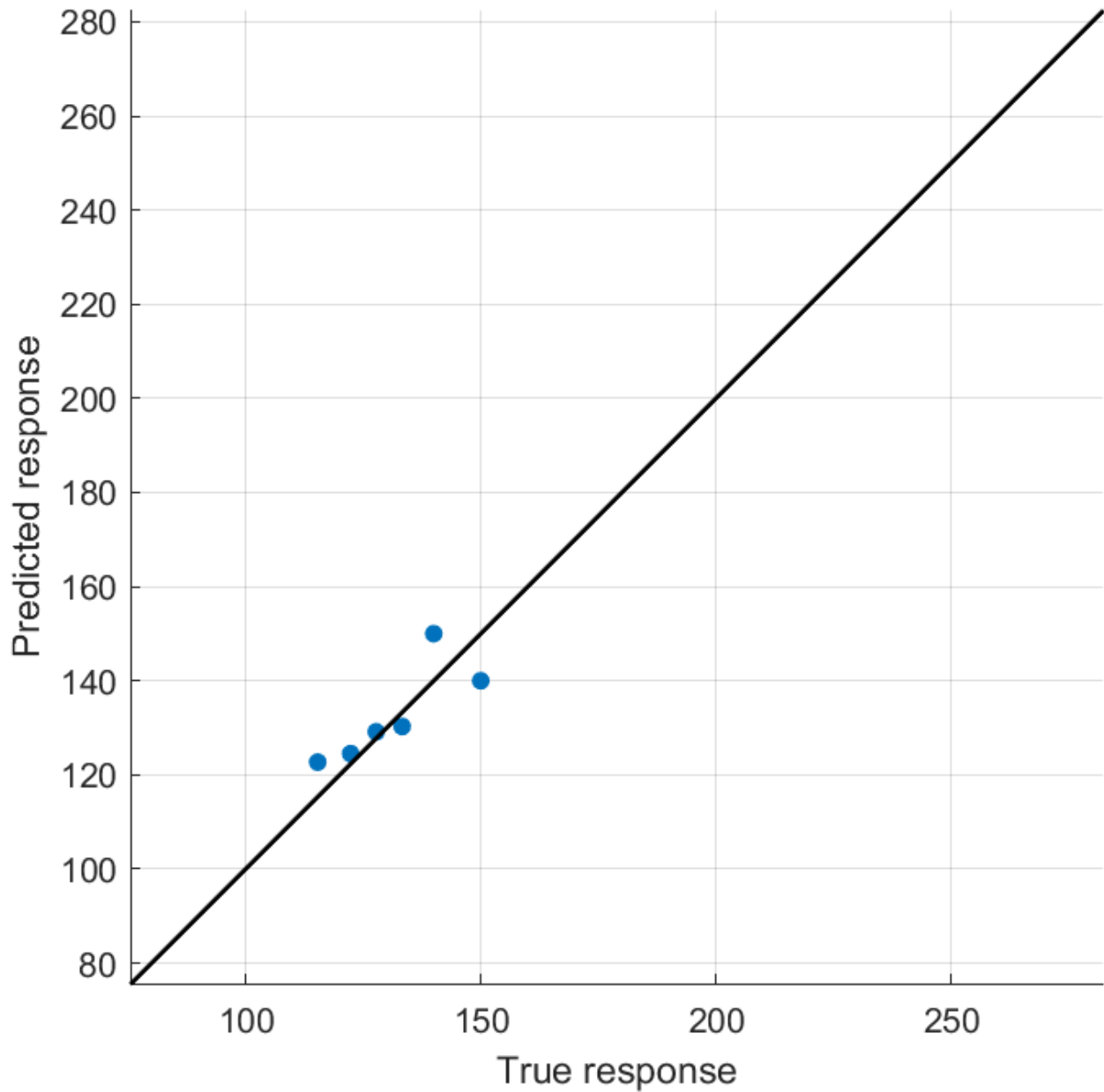


Figure S1. Linear Regression (RMSE: 6.7095, R^2 : 0.98) – This is the multiple linear regression model generated for size related data.

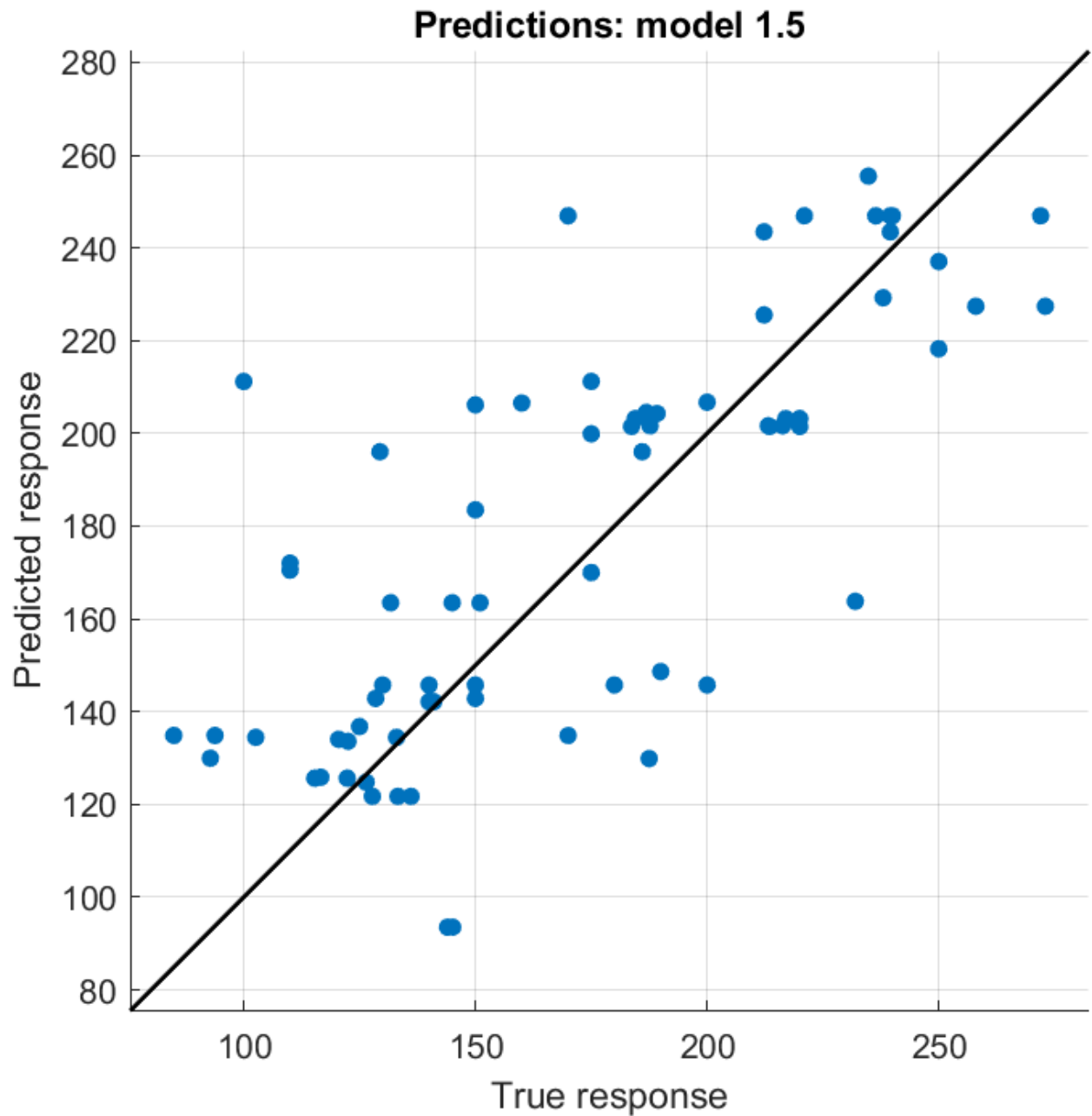


Figure S2. Fine Tree Model (RMSE: 32.863, R^2 :0.56) – This is the fine decision tree model for size related data. This model was eventually discarded for its inability to respond to variation of input stimuli.

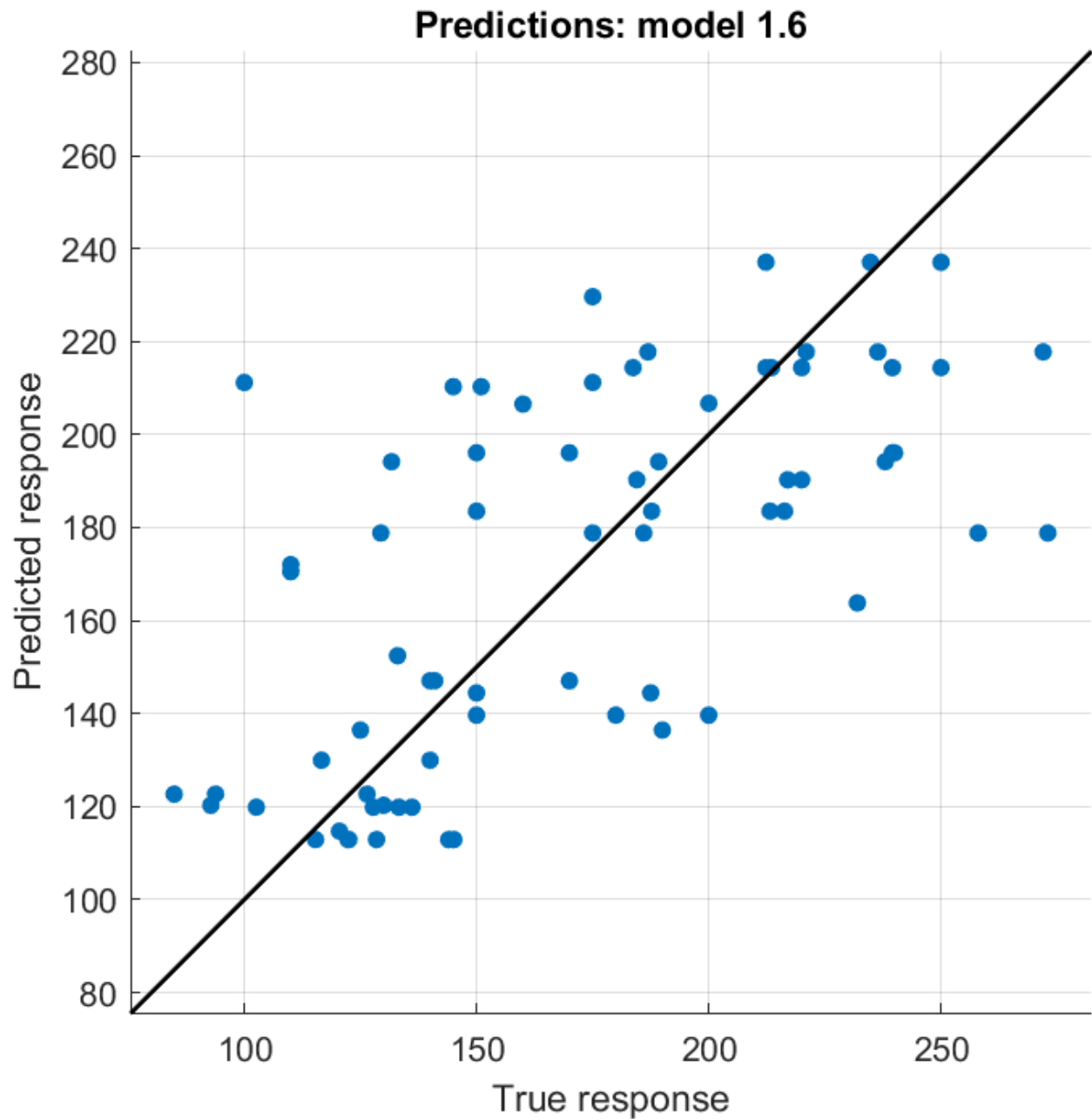


Figure S3. Medium Tree Model (RMSE: 36.944, R^2 : 0.45) - This is the medium decision tree model for size related data. This model was eventually discarded for its inability to respond to variation of input stimuli.

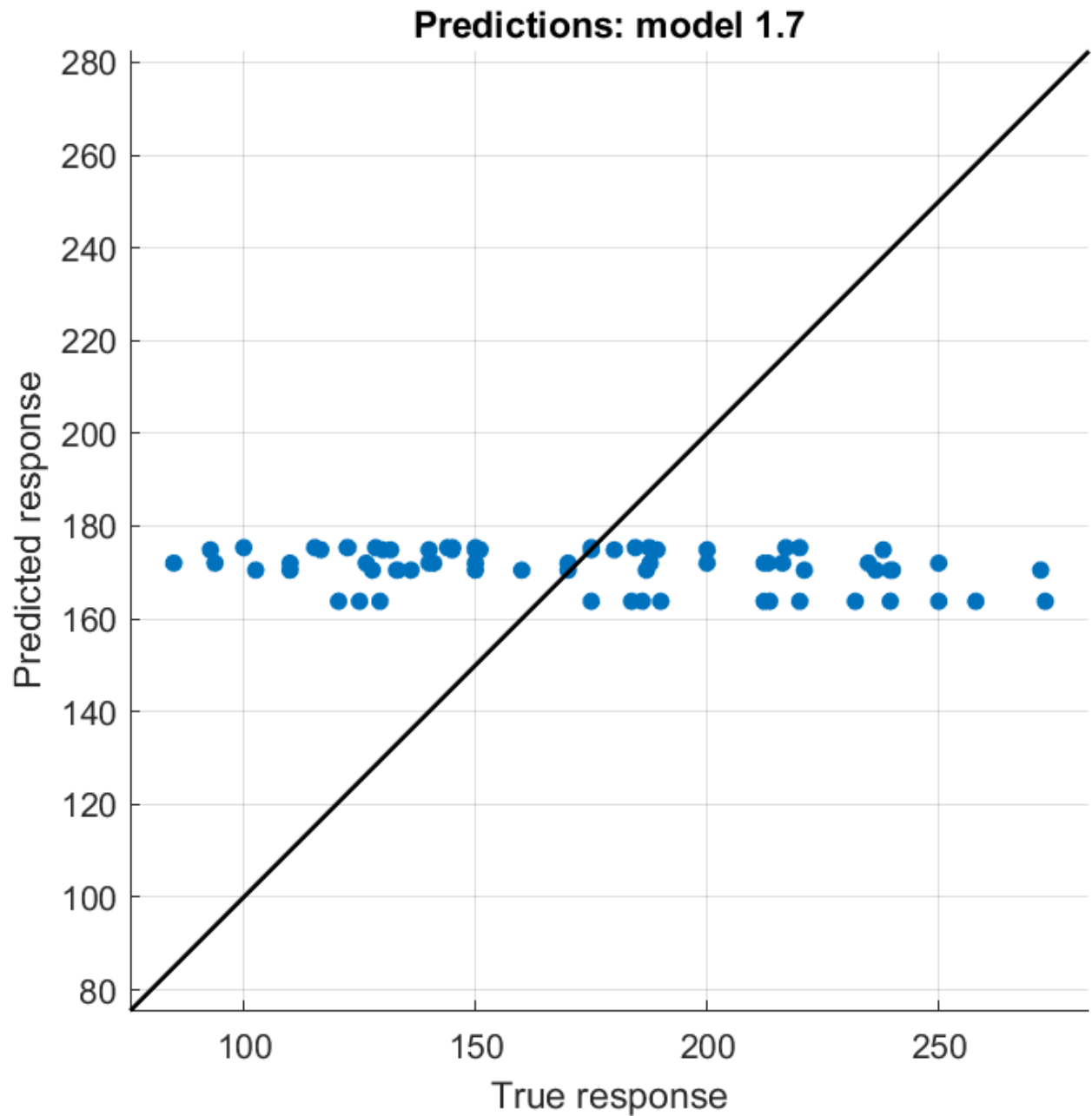


Figure S4. Coarse Tree Model (RMSE: 49.654, R^2 : 0.00) - This is the coarse decision tree model for size related data. This model was eventually discarded for its inability to respond to variation of input stimuli.

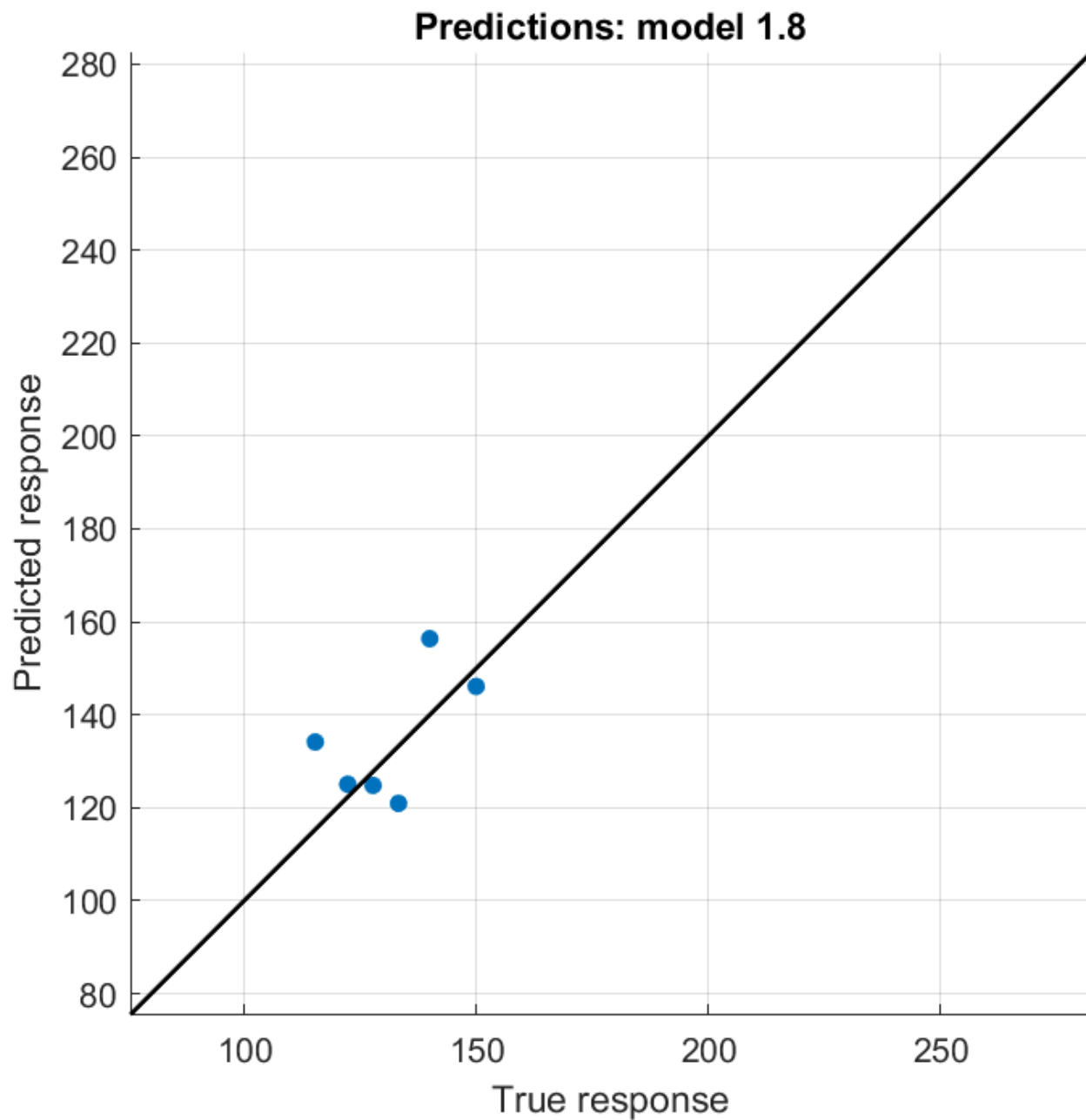


Figure S5. Linear SVM (RMSE:11.581, R^2 : 0.93) – linear support vector machine

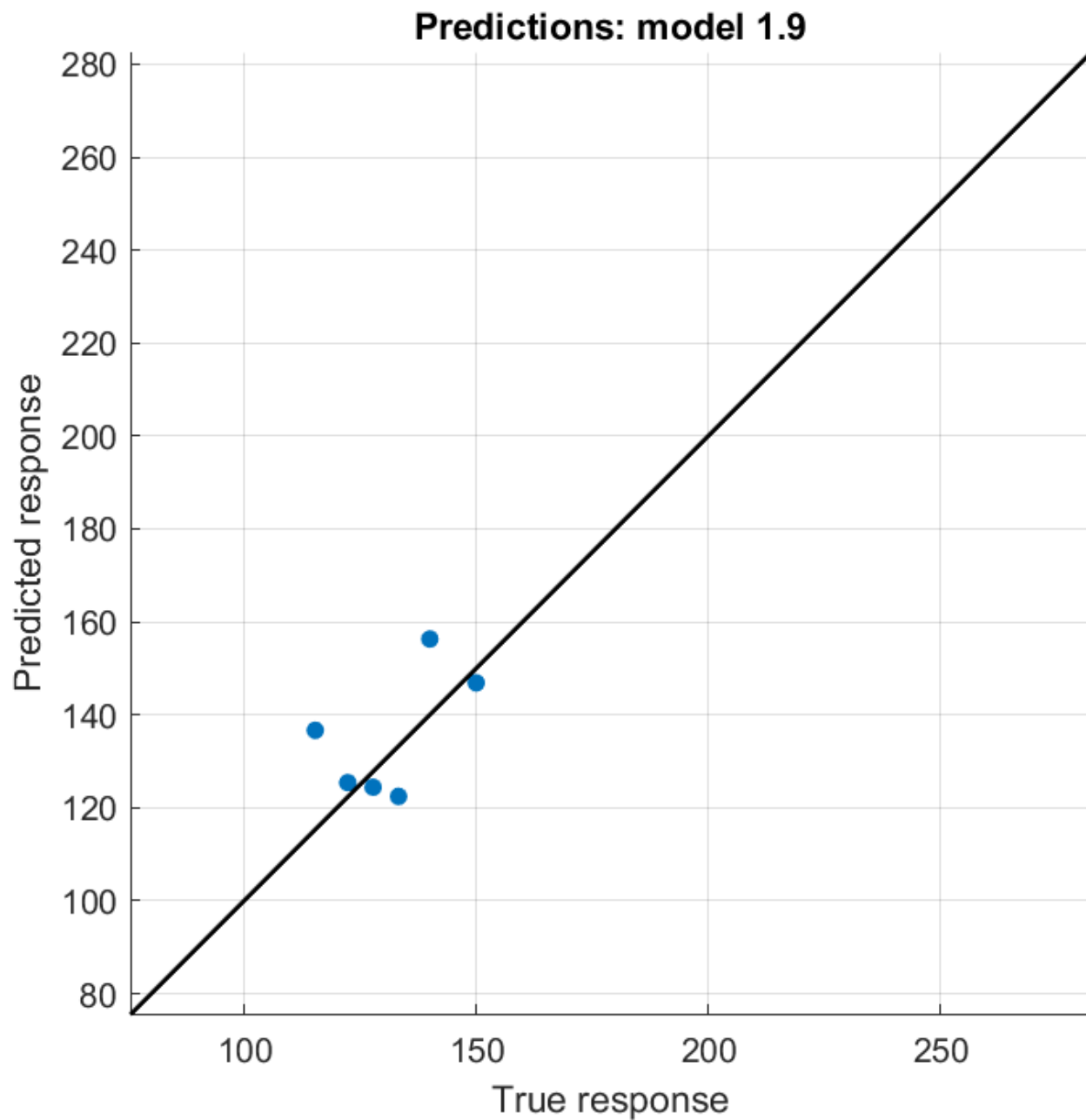


Figure S6. Quadratic SVM (RMSE:12.048, R^2 : 0.92) – Quadratic Support Vector Machine

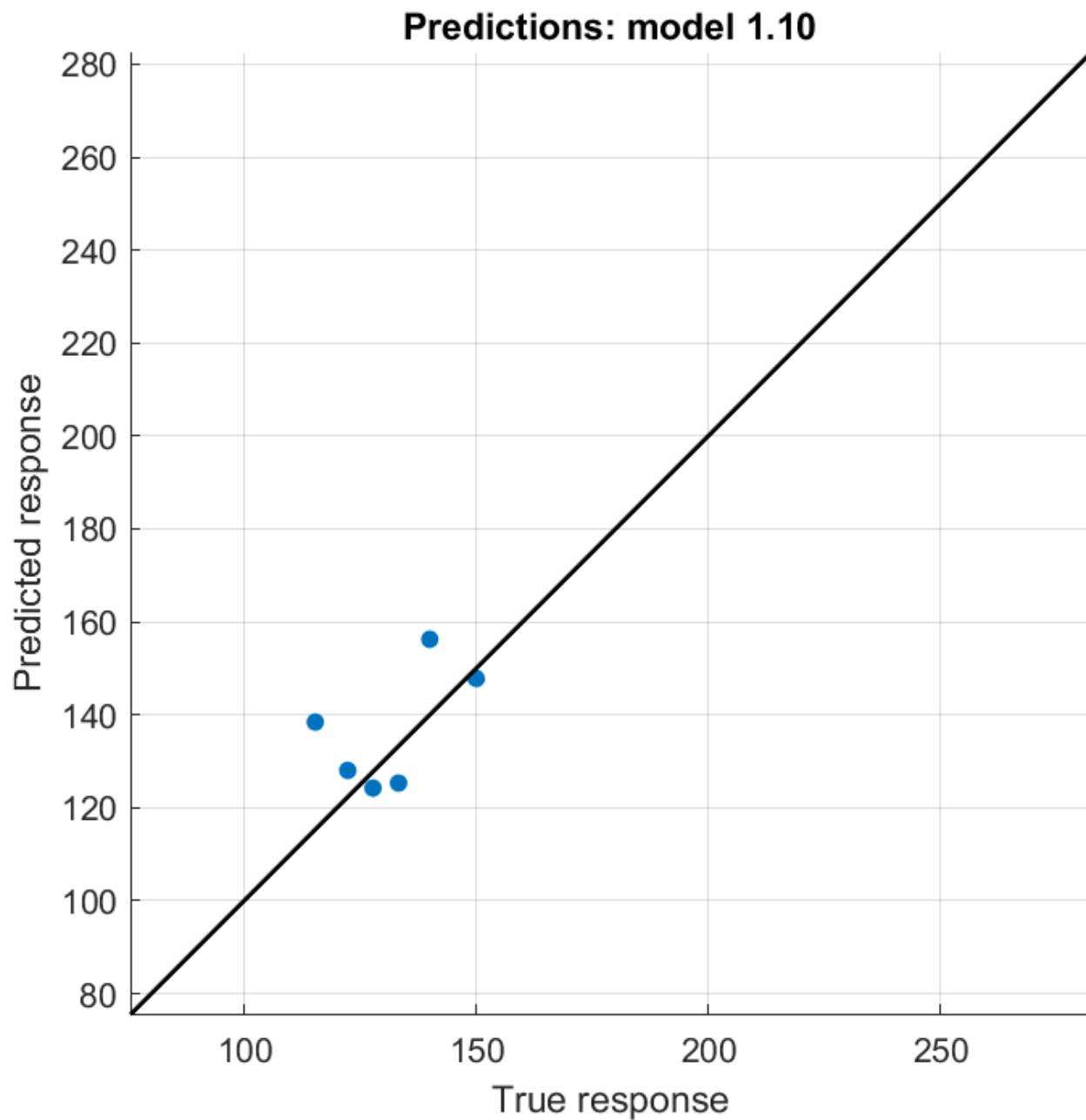


Figure S7. Cubic SVM (RMSE: 12.291, R^2 : 0.92) – Cubic Support Vector Machine

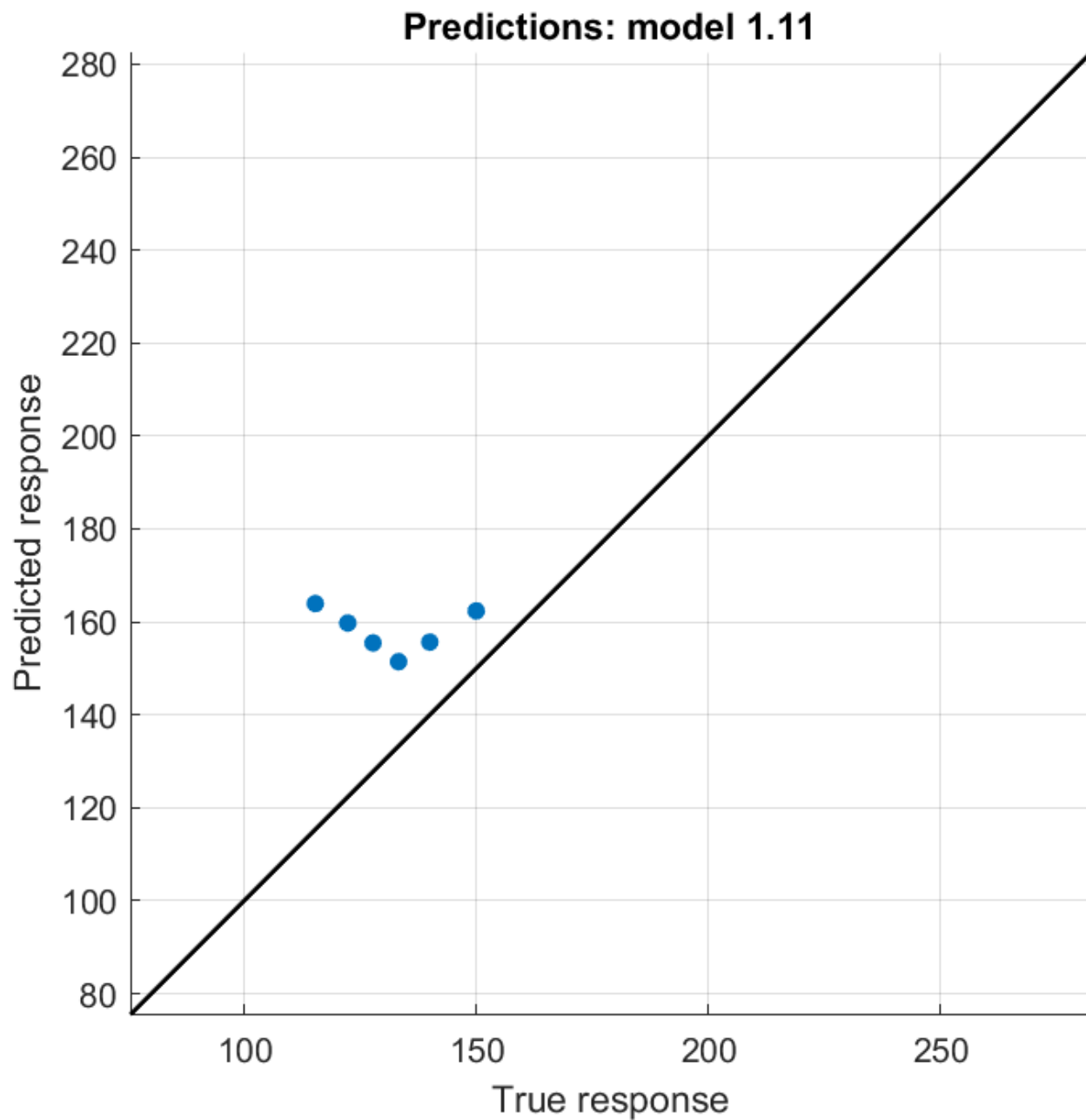


Figure S8. Fine Gaussian SVM (RMSE: 29.602, R^2 : 0.53)

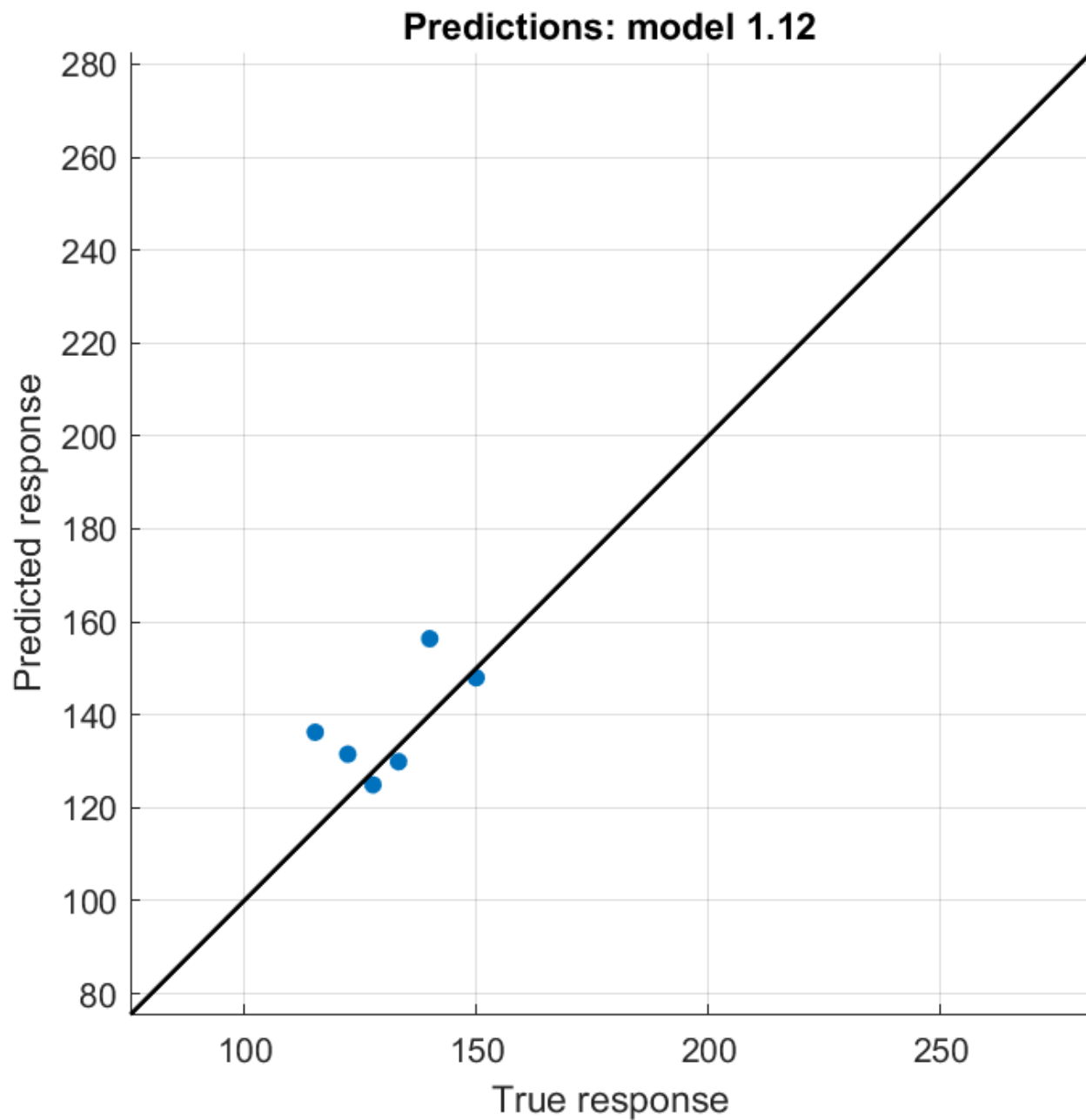


Figure S9. Medium Gaussian SVM (RMSE: 11.651, R^2 : 0.93)

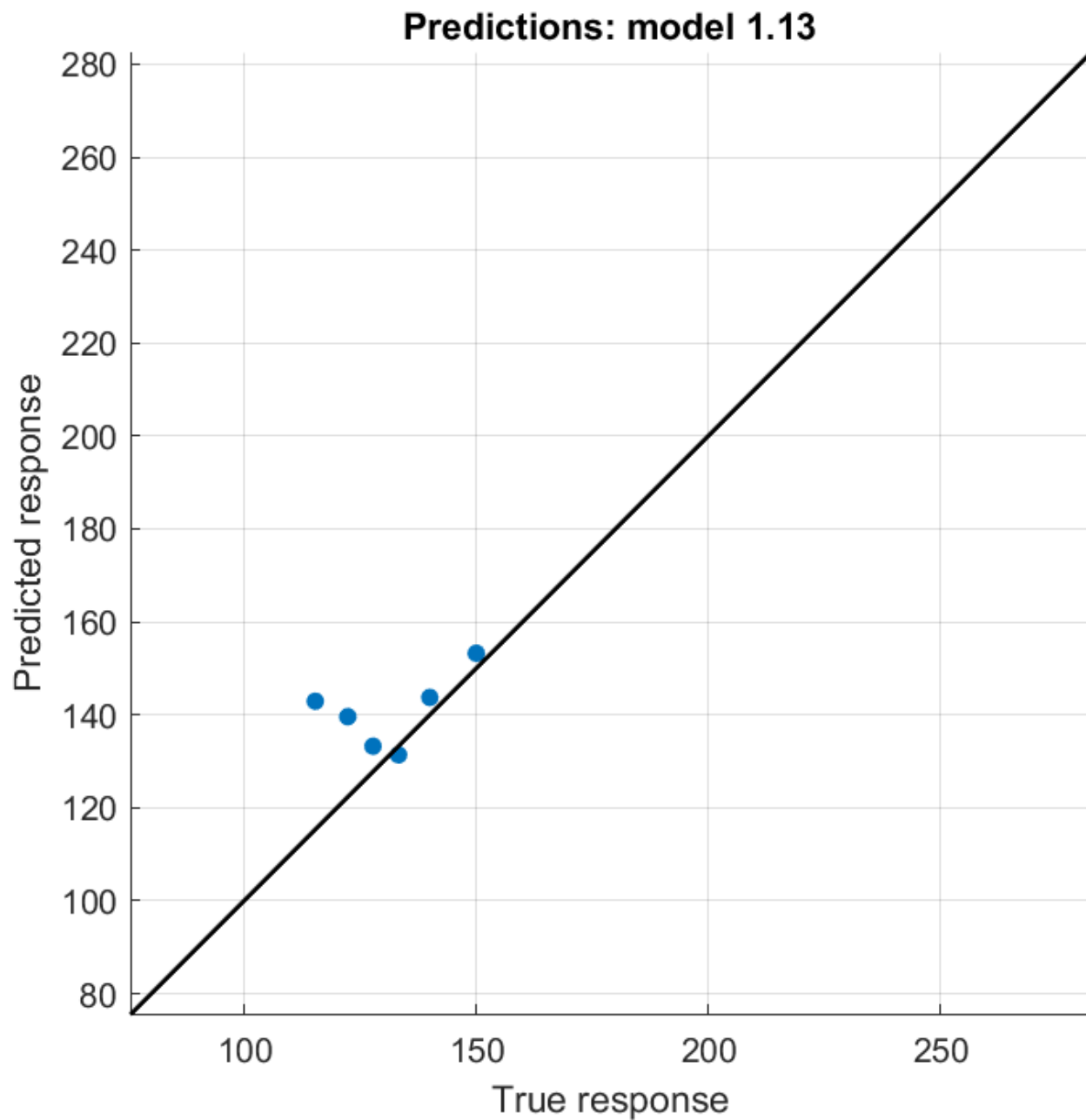


Figure S10. Coarse Gaussian SVM (RMSE:13.649, R^2 : 0.90)

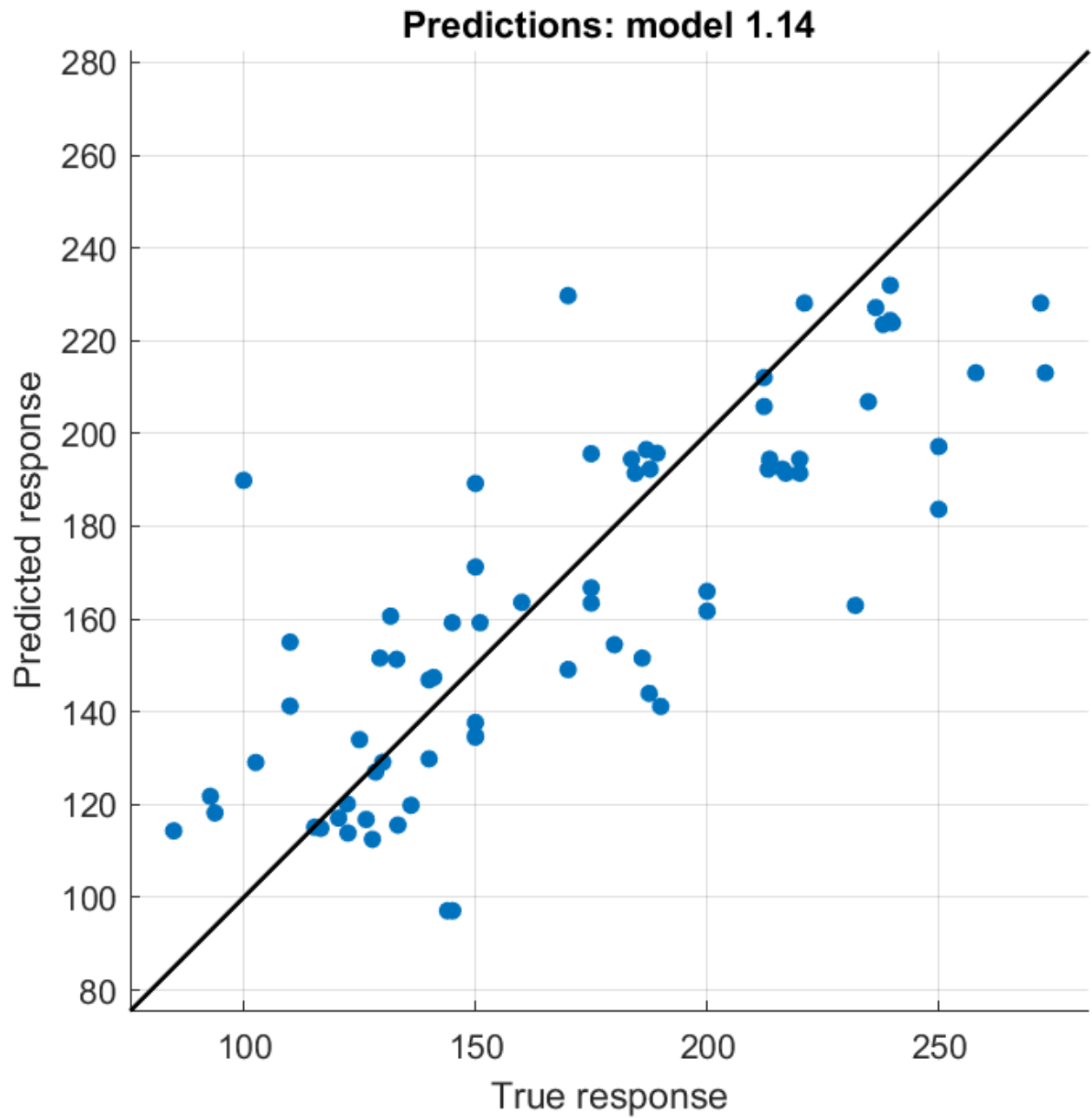


Figure S11. Boosted Tree (RMSE:29.37, R^2 : 0.65)

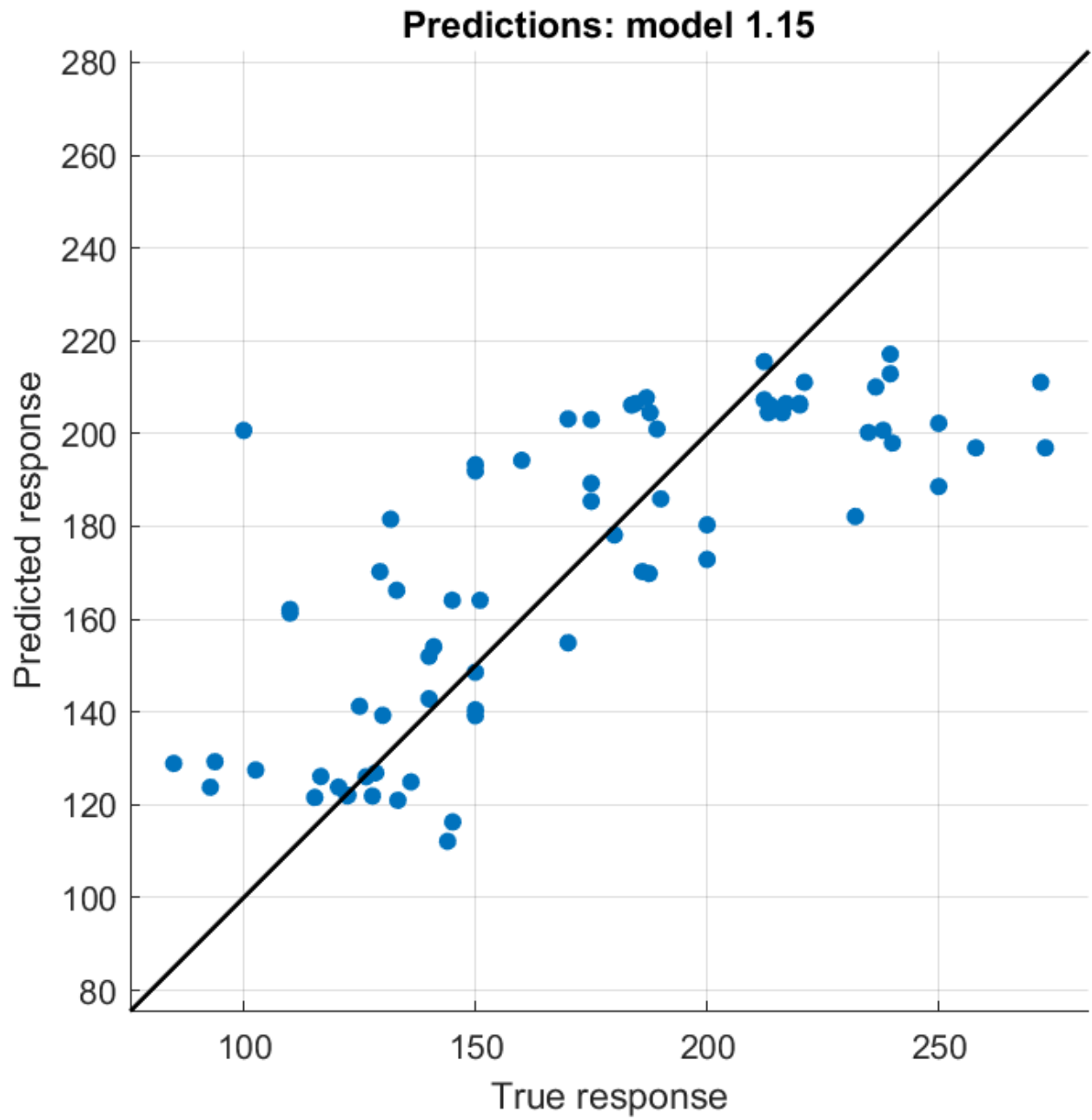


Figure S12. Bagged Tree (RMSE: 30.261, R^2 : 0.63)

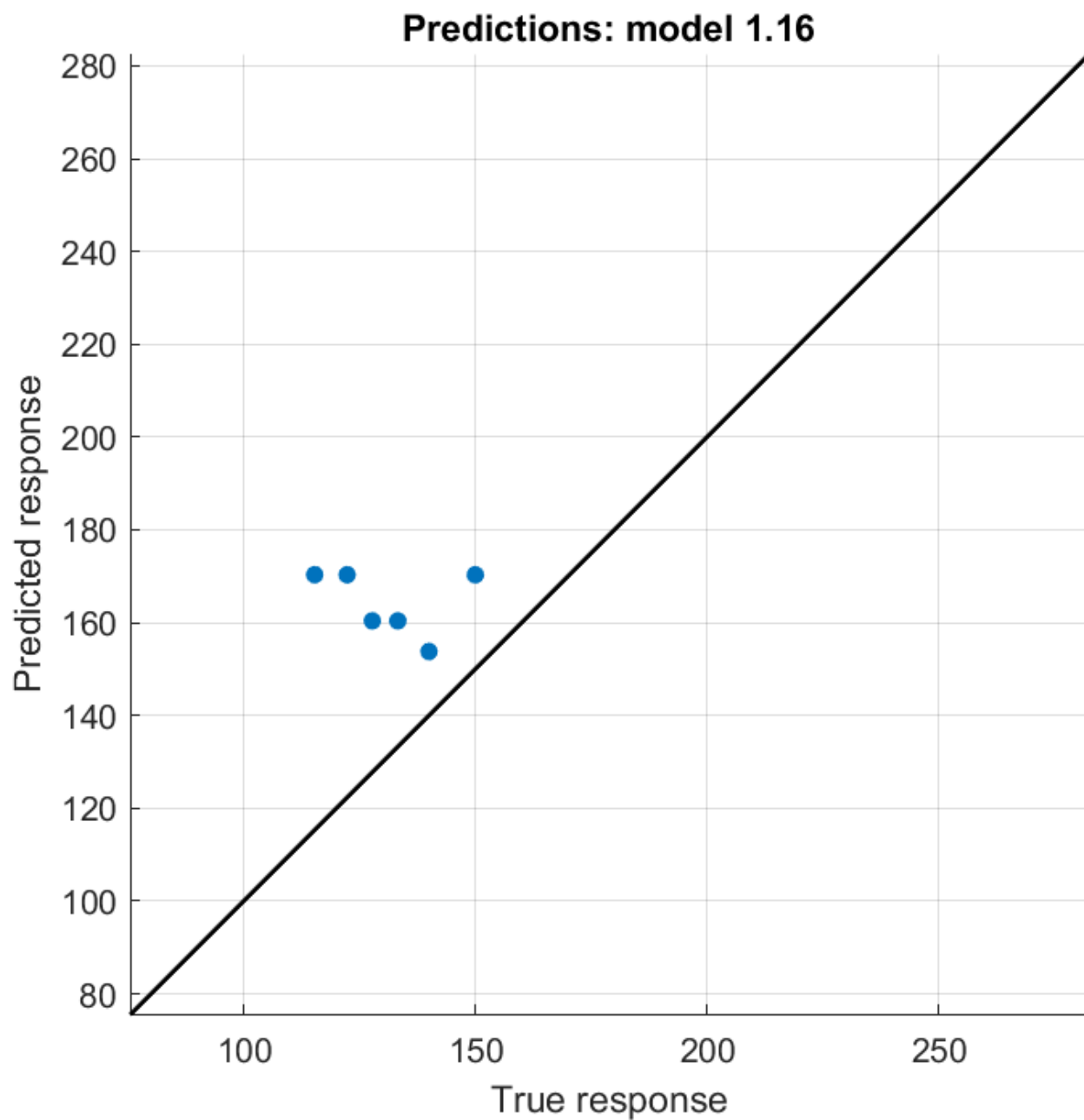


Figure S13. Squared Exponential GPR (RMSE: 35.888, R^2 : 0.32)

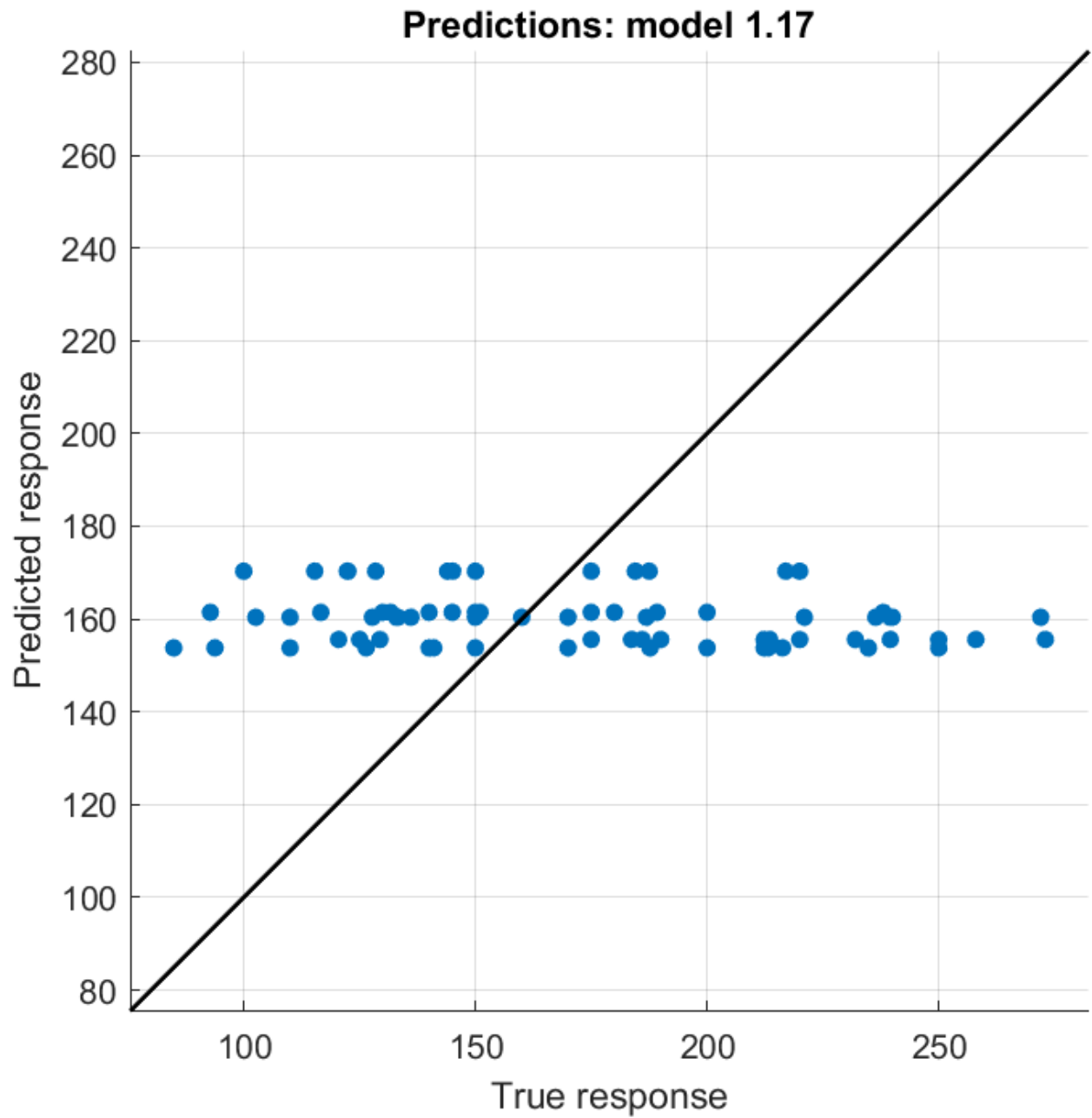


Figure S14. Matern 5/2 GPR (RMSE: 50.875, R^2 : -0.05) – Gaussian Process Regression

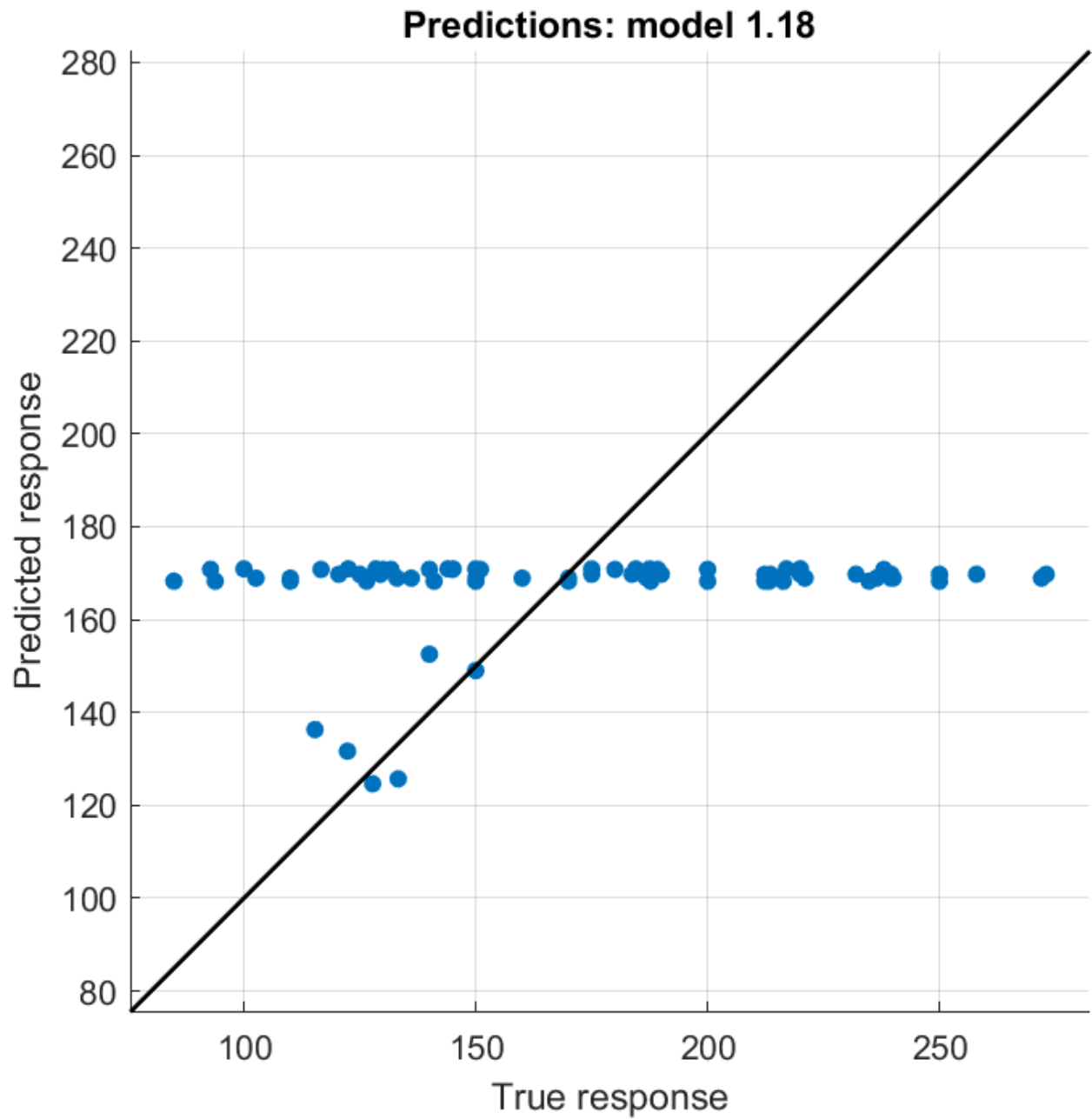


Figure S15. Exponential GPR (RMSE: 46.948, R^2 : 0.11) – Gaussian Process Regression

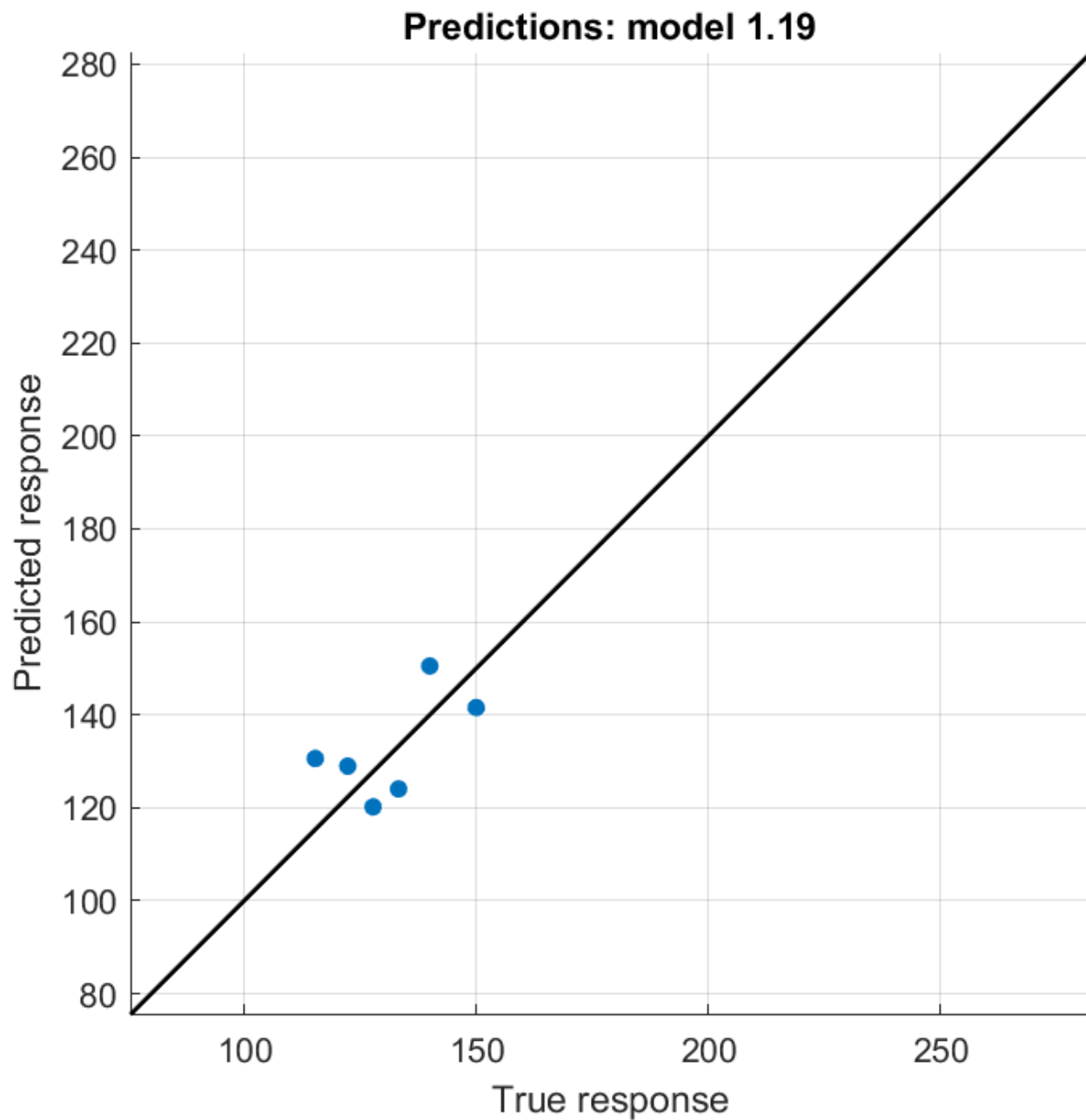


Figure S16. Rational Quadratic GPR (RMSE:10.013, R^2 : 0.95) – Gaussian Process Regression

References

1. Ragaller, M. & Richter, T. Acute lung injury and acute respiratory distress syndrome. *J. Emerg. Trauma Shock* **3**, 43–51 (2010).
2. Matthay, M. A. *et al.* Acute respiratory distress syndrome. *Nat. Rev. Dis. Primer* **5**, 18 (2019).
3. ARDS Definition Task Force *et al.* Acute respiratory distress syndrome: the Berlin Definition. *JAMA* **307**, 2526–2533 (2012).
4. Rubenfeld, G. D. *et al.* Incidence and Outcomes of Acute Lung Injury. *N. Engl. J. Med.* **353**, 1685–1693 (2005).
5. Bellani, G. *et al.* Epidemiology, Patterns of Care, and Mortality for Patients With Acute Respiratory Distress Syndrome in Intensive Care Units in 50 Countries. *JAMA* **315**, 788 (2016).
6. Cortegiani, A. *et al.* Immunocompromised patients with acute respiratory distress syndrome: secondary analysis of the LUNG SAFE database. *Crit. Care Lond. Engl.* **22**, 157 (2018).
7. Toy, P. *et al.* Transfusion-related acute lung injury: incidence and risk factors. *Blood* **119**, 1757–1767 (2012).
8. Crimi, E. & Slutsky, A. S. Inflammation and the acute respiratory distress syndrome. *Best Pract. Res. Clin. Anaesthesiol.* **18**, 477–492 (2004).
9. Acute Respiratory Distress Syndrome Network *et al.* Ventilation with lower tidal volumes as compared with traditional tidal volumes for acute lung injury and the acute respiratory distress syndrome. *N. Engl. J. Med.* **342**, 1301–1308 (2000).
10. Butt, Y., Kurdowska, A. & Allen, T. C. Acute Lung Injury: A Clinical and Molecular Review. *Arch. Pathol. Lab. Med.* **140**, 345–350 (2016).
11. Zhu, L., Li, M., Dong, J. & Jin, Y. Dimethyl silicone dry nanoemulsion inhalations: Formulation study and anti-acute lung injury effect. *Int. J. Pharm.* **491**, 292–298 (2015).
12. Leaver, S. K. & Evans, T. W. Acute respiratory distress syndrome. *BMJ* **335**, 389–394 (2007).
13. Park, W. Y. *et al.* Cytokine balance in the lungs of patients with acute respiratory distress syndrome. *Am. J. Respir. Crit. Care Med.* **164**, 1896–1903 (2001).

14. Steinberg, K. P. *et al.* Evolution of bronchoalveolar cell populations in the adult respiratory distress syndrome. *Am. J. Respir. Crit. Care Med.* **150**, 113–122 (1994).
15. Adhikari, N., Burns, K. E. A. & Meade, M. O. Pharmacologic therapies for adults with acute lung injury and acute respiratory distress syndrome. *Cochrane Database Syst. Rev.* CD004477 (2004) doi:10.1002/14651858.CD004477.pub2.
16. Anzueto, A. *et al.* Aerosolized surfactant in adults with sepsis-induced acute respiratory distress syndrome. Exosurf Acute Respiratory Distress Syndrome Sepsis Study Group. *N. Engl. J. Med.* **334**, 1417–1421 (1996).
17. Taylor, R. W. *et al.* Low-dose inhaled nitric oxide in patients with acute lung injury: a randomized controlled trial. *JAMA* **291**, 1603–1609 (2004).
18. Ketoconazole for early treatment of acute lung injury and acute respiratory distress syndrome: a randomized controlled trial. The ARDS Network. *JAMA* **283**, 1995–2002 (2000).
19. Jepsen, S., Herlevsen, P., Knudsen, P., Bud, M. I. & Klausen, N. O. Antioxidant treatment with N-acetylcysteine during adult respiratory distress syndrome: a prospective, randomized, placebo-controlled study. *Crit. Care Med.* **20**, 918–923 (1992).
20. Khilnani, G. C. & Hadda, V. Corticosteroids and ARDS: A review of treatment and prevention evidence. *Lung India Off. Organ Indian Chest Soc.* **28**, 114–119 (2011).
21. Baldwin, Stephen R. *et al.* OXIDANT ACTIVITY IN EXPIRED BREATH OF PATIENTS WITH ADULT RESPIRATORY DISTRESS SYNDROME. *The Lancet* **327**, 11–14 (1986).
22. Lykens, M. G., Davis, W. B. & Pacht, E. R. Antioxidant activity of bronchoalveolar lavage fluid in the adult respiratory distress syndrome. *Am. J. Physiol.* **262**, L169-175 (1992).
23. Takeda, K. *et al.* Plasma lipid peroxides and alpha-tocopherol in critically ill patients. *Crit. Care Med.* **12**, 957–959 (1984).
24. Leff, J. A. *et al.* Serum antioxidants as predictors of adult respiratory distress syndrome in patients with sepsis. *Lancet Lond. Engl.* **341**, 777–780 (1993).

25. Bernard, G. R. *et al.* A trial of antioxidants N-acetylcysteine and procysteine in ARDS. The Antioxidant in ARDS Study Group. *Chest* **112**, 164–172 (1997).
26. Donnelly, S. C. & Robertson, C. Trauma, inflammatory cells and ARDS. *Arch. Emerg. Med.* **10**, 108–111 (1993).
27. Ahrens, E. T. & Bulte, J. W. M. Tracking immune cells in vivo using magnetic resonance imaging. *Nat. Rev. Immunol.* **13**, 755–763 (2013).
28. Ebner, B. *et al.* Early Assessment of Pulmonary Inflammation By ¹⁹F MRI In Vivo. *Circ. Cardiovasc. Imaging* **3**, 202–210 (2010).
29. Fox, M. S., Gaudet, J. M. & Foster, P. J. Fluorine-19 MRI Contrast Agents for Cell Tracking and Lung Imaging. *Magn. Reson. Insights* **8**, 53–67 (2016).
30. Janjic, J. M. & Ahrens, E. T. Fluorine-containing nanoemulsions for MRI cell tracking. *Wiley Interdiscip. Rev. Nanomed. Nanobiotechnol.* **1**, 492–501 (2009).
31. Ahrens, E. T. & Zhong, J. In vivo MRI cell tracking using perfluorocarbon probes and fluorine-19 detection. *NMR Biomed.* **26**, 860–871 (2013).
32. Jain, K. K. *The handbook of nanomedicine.* (Humana Press, 2017).
33. Singh, A. P., Biswas, A., Shukla, A. & Maiti, P. Targeted therapy in chronic diseases using nanomaterial-based drug delivery vehicles. *Signal Transduct. Target. Ther.* **4**, 1–21 (2019).
34. Janjic, J. M. *et al.* Low-dose NSAIDs reduce pain via macrophage targeted nanoemulsion delivery to neuroinflammation of the sciatic nerve in rat. *J. Neuroimmunol.* **318**, 72–79 (2018).
35. Bakry, R. *et al.* Medicinal applications of fullerenes. *Int. J. Nanomedicine* **2**, 639–649 (2007).
36. Kazemzadeh, H. & Mozafari, M. Fullerene-based delivery systems. *Drug Discov. Today* **24**, 898–905 (2019).
37. Pardeike, J., Hommoss, A. & Müller, R. H. Lipid nanoparticles (SLN, NLC) in cosmetic and pharmaceutical dermal products. *Int. J. Pharm.* **366**, 170–184 (2009).
38. García-Pinel, B. *et al.* Lipid-Based Nanoparticles: Application and Recent Advances in Cancer Treatment. *Nanomaterials* **9**, (2019).

39. Mishra, V. *et al.* Solid Lipid Nanoparticles: Emerging Colloidal Nano Drug Delivery Systems. *Pharmaceutics* **10**, (2018).
40. S.A, R. K. H. J. Solid Lipid Nanoparticle: A Review. in (2012). doi:10.9790/3013-26103444.
41. Costa, A., Sarmiento, B. & Seabra, V. Mannose-functionalized solid lipid nanoparticles are effective in targeting alveolar macrophages. *Eur. J. Pharm. Sci. Off. J. Eur. Fed. Pharm. Sci.* **114**, 103–113 (2018).
42. Müller, R. H., Radtke, M. & Wissing, S. A. Nanostructured lipid matrices for improved microencapsulation of drugs. *Int. J. Pharm.* **242**, 121–128 (2002).
43. Fang, G. *et al.* Cysteine-Functionalized Nanostructured Lipid Carriers for Oral Delivery of Docetaxel: A Permeability and Pharmacokinetic Study. *Mol. Pharm.* **12**, 2384–2395 (2015).
44. Singh, S. K. *et al.* Glycol chitosan functionalized asenapine nanostructured lipid carriers for targeted brain delivery: Pharmacokinetic and teratogenic assessment. *Int. J. Biol. Macromol.* **108**, 1092–1100 (2018).
45. de Gennaro, B. Chapter 3 - Surface modification of zeolites for environmental applications. in *Modified Clay and Zeolite Nanocomposite Materials* (eds. Mercurio, M., Sarkar, B. & Langella, A.) 57–85 (Elsevier, 2019). doi:10.1016/B978-0-12-814617-0.00009-8.
46. Croy, S. & Kwon, G. Polymeric Micelles for Drug Delivery. *Curr. Pharm. Des.* **12**, 4669–4684 (2006).
47. Zhang, Y., Huang, Y. & Li, S. Polymeric Micelles: Nanocarriers for Cancer-Targeted Drug Delivery. *AAPS PharmSciTech* **15**, 862–871 (2014).
48. Kwon, G. S. & Okano, T. Polymeric micelles as new drug carriers. *Adv. Drug Deliv. Rev.* **21**, 107–116 (1996).
49. Geng, Y. *et al.* Shape effects of filaments versus spherical particles in flow and drug delivery. *Nat. Nanotechnol.* **2**, 249–255 (2007).
50. Bera, D., Qian, L., Tseng, T.-K. & Holloway, P. H. Quantum Dots and Their Multimodal Applications: A Review. *Materials* **3**, 2260–2345 (2010).

51. Zhao, M.-X. & Zhu, B.-J. The Research and Applications of Quantum Dots as Nano-Carriers for Targeted Drug Delivery and Cancer Therapy. *Nanoscale Res. Lett.* **11**, 207 (2016).
52. Bailey, R. E., Smith, A. M. & Nie, S. Quantum dots in biology and medicine. *Phys. E Low-Dimens. Syst. Nanostructures* **25**, 1–12 (2004).
53. Paranjpe, M. & Müller-Goymann, C. C. Nanoparticle-Mediated Pulmonary Drug Delivery: A Review. *Int. J. Mol. Sci.* **15**, 5852–5873 (2014).
54. Beck-Broichsitter, M., Schmehl, T., Gessler, T., Seeger, W. & Kissel, T. Development of a biodegradable nanoparticle platform for sildenafil: formulation optimization by factorial design analysis combined with application of charge-modified branched polyesters. *J. Control. Release Off. J. Control. Release Soc.* **157**, 469–477 (2012).
55. Beck-Broichsitter, M., Ruppert, C., Schmehl, T., Günther, A. & Seeger, W. Biophysical inhibition of synthetic vs. naturally-derived pulmonary surfactant preparations by polymeric nanoparticles. *Biochim. Biophys. Acta* **1838**, 474–481 (2014).
56. Lee, B. K., Yun, Y. & Park, K. PLA Micro- and Nano-Particles. *Adv. Drug Deliv. Rev.* **107**, 176–191 (2016).
57. Shive, null & Anderson, null. Biodegradation and biocompatibility of PLA and PLGA microspheres. *Adv. Drug Deliv. Rev.* **28**, 5–24 (1997).
58. Soppimath, K. S., Aminabhavi, T. M., Kulkarni, A. R. & Rudzinski, W. E. Biodegradable polymeric nanoparticles as drug delivery devices. *J. Control. Release Off. J. Control. Release Soc.* **70**, 1–20 (2001).
59. Bhavsar, M. D. & Amiji, M. M. Development of Novel Biodegradable Polymeric Nanoparticles-in-Microsphere Formulation for Local Plasmid DNA Delivery in the Gastrointestinal Tract. *AAPS PharmSciTech* **9**, 288–294 (2008).
60. Menon, J. U. *et al.* Polymeric Nanoparticles for Pulmonary Protein and DNA Delivery. *Acta Biomater.* **10**, 2643–2652 (2014).

61. Abd Ellah, N. H. & Abouelmagd, S. A. Surface functionalization of polymeric nanoparticles for tumor drug delivery: approaches and challenges. *Expert Opin. Drug Deliv.* **14**, 201–214 (2017).
62. Sham, J. O.-H., Zhang, Y., Finlay, W. H., Roa, W. H. & Löbenberg, R. Formulation and characterization of spray-dried powders containing nanoparticles for aerosol delivery to the lung. *Int. J. Pharm.* **269**, 457–467 (2004).
63. Sung, J. C., Pulliam, B. L. & Edwards, D. A. Nanoparticles for drug delivery to the lungs. *Trends Biotechnol.* **25**, 563–570 (2007).
64. Nesamony, J., Singh, P. R., Nada, S. E., Shah, Z. A. & Kolling, W. M. Calcium alginate nanoparticles synthesized through a novel interfacial cross-linking method as a potential protein drug delivery system. *J. Pharm. Sci.* **101**, 2177–2184 (2012).
65. Yadav, H. K. S., Almokdad, A. A., shaluf, S. I. M. & Debe, M. S. Chapter 17 - Polymer-Based Nanomaterials for Drug-Delivery Carriers. in *Nanocarriers for Drug Delivery* (eds. Mohapatra, S. S., Ranjan, S., Dasgupta, N., Mishra, R. K. & Thomas, S.) 531–556 (Elsevier, 2019). doi:10.1016/B978-0-12-814033-8.00017-5.
66. Egusquiaguirre, S. P., Pedraz, J. L., Hernández, R. M. & Igartua, M. 29 - Nanotherapeutic Platforms for Cancer Treatment: From Preclinical Development to Clinical Application. in *Nanoarchitectonics for Smart Delivery and Drug Targeting* (eds. Holban, A. M. & Grumezescu, A. M.) 813–869 (William Andrew Publishing, 2016). doi:10.1016/B978-0-323-47347-7.00029-X.
67. Enrico, C. Chapter 2 - Nanotheranostics and theranostic nanomedicine for diseases and cancer treatment. in *Design of Nanostructures for Theranostics Applications* (ed. Grumezescu, A. M.) 41–68 (William Andrew Publishing, 2018). doi:10.1016/B978-0-12-813669-0.00002-6.
68. Madaan, K., Kumar, S., Poonia, N., Lather, V. & Pandita, D. Dendrimers in drug delivery and targeting: Drug-dendrimer interactions and toxicity issues. *J. Pharm. Bioallied Sci.* **6**, 139–150 (2014).

69. Soto-Castro, D., Cruz-Morales, J. A., Ramírez Apan, M. T. & Guadarrama, P. Solubilization and anticancer-activity enhancement of Methotrexate by novel dendrimeric nanodevices synthesized in one-step reaction. *Bioorganic Chem.* **41–42**, 13–21 (2012).
70. Duncan, R. & Izzo, L. Dendrimer biocompatibility and toxicity. *Adv. Drug Deliv. Rev.* **57**, 2215–2237 (2005).
71. Tomalia, D. A. Birth of a new macromolecular architecture: dendrimers as quantized building blocks for nanoscale synthetic polymer chemistry. *Prog. Polym. Sci.* **30**, 294–324 (2005).
72. Vögtle, F. & Astruc, D. *Dendrimers II: Architecture, Nanostructure and Supramolecular Chemistry*. (Springer Science & Business Media, 2000).
73. Astruc, D., Boisselier, E. & Ornelas, C. Dendrimers Designed for Functions: From Physical, Photophysical, and Supramolecular Properties to Applications in Sensing, Catalysis, Molecular Electronics, Photonics, and Nanomedicine. *Chem. Rev.* **110**, 1857–1959 (2010).
74. Kitchens, K. M., El-Sayed, M. E. H. & Ghandehari, H. Transepithelial and endothelial transport of poly (amidoamine) dendrimers. *Adv. Drug Deliv. Rev.* **57**, 2163–2176 (2005).
75. Ghosh, P. & Murthy, R. Microemulsions: A Potential Drug Delivery System. *Curr. Drug Deliv.* **3**, 167–180 (2006).
76. Abdul Rahman, M. B. *et al.* Chapter 6 - Palm-based nanoemulsions for drug delivery systems. in *Organic Materials as Smart Nanocarriers for Drug Delivery* (ed. Grumezescu, A. M.) 209–244 (William Andrew Publishing, 2018). doi:10.1016/B978-0-12-813663-8.00006-3.
77. Qadir, A., Faiyazuddin, M. D., Talib Hussain, M. D., Alshammari, T. M. & Shakeel, F. Critical steps and energetics involved in a successful development of a stable nanoemulsion. *J. Mol. Liq.* **214**, 7–18 (2016).
78. Lambert, E., Gorantla, V. S. & Janjic, J. M. Pharmaceutical design and development of perfluorocarbon nanocolloids for oxygen delivery in regenerative medicine. *Nanomed.* **14**, 2697–2712 (2019).

79. Patel, S. K., Patrick, M. J., Pollock, J. A. & Janjic, J. M. Two-color fluorescent (near-infrared and visible) triphasic perfluorocarbon nanoemulsions. *J. Biomed. Opt.* **18**, 101312 (2013).
80. Sengel-Turk, C. T., Gumustas, M., Uslu, B. & Ozkan, S. A. Chapter 10 - Nanosized Drug Carriers for Oral Delivery of Anticancer Compounds and the Importance of the Chromatographic Techniques. in *Nano- and Microscale Drug Delivery Systems* (ed. Grumezescu, A. M.) 165–195 (Elsevier, 2017). doi:10.1016/B978-0-323-52727-9.00010-8.
81. Bulbake, U., Doppalapudi, S., Kommineni, N. & Khan, W. Liposomal Formulations in Clinical Use: An Updated Review. *Pharmaceutics* **9**, (2017).
82. Akbarzadeh, A. *et al.* Liposome: classification, preparation, and applications. *Nanoscale Res. Lett.* **8**, 102 (2013).
83. Palankar, R., Ramaye, Y., Fournier, D. & Winterhalter, M. Chapter 2 Functionalized Liposomes. in *Advances in Planar Lipid Bilayers and Liposomes* vol. 7 39–58 (Academic Press, 2008).
84. Vabbilisetty, P. & Sun, X.-L. Liposome Surface Functionalization Based on Different Anchoring Lipids via Staudinger Ligation. *Org. Biomol. Chem.* **12**, 1237–1244 (2014).
85. Han, S. & Mallampalli, R. K. The acute respiratory distress syndrome: from mechanism to translation. *J. Immunol. Baltim. Md 1950* **194**, 855–860 (2015).
86. Peter, J. V. *et al.* Corticosteroids in the prevention and treatment of acute respiratory distress syndrome (ARDS) in adults: meta-analysis. *BMJ* **336**, 1006–1009 (2008).
87. Iwata, K. *et al.* Effect of neutrophil elastase inhibitor (sivelestat sodium) in the treatment of acute lung injury (ALI) and acute respiratory distress syndrome (ARDS): a systematic review and meta-analysis. *Intern. Med. Tokyo Jpn.* **49**, 2423–2432 (2010).
88. Paine, R. *et al.* A randomized trial of recombinant human granulocyte-macrophage colony stimulating factor for patients with acute lung injury. *Crit. Care Med.* **40**, 90–97 (2012).
89. National Heart, Lung, and Blood Institute ARDS Clinical Trials Network *et al.* Rosuvastatin for sepsis-associated acute respiratory distress syndrome. *N. Engl. J. Med.* **370**, 2191–2200 (2014).

90. Rice, T. W. *et al.* Enteral omega-3 fatty acid, gamma-linolenic acid, and antioxidant supplementation in acute lung injury. *JAMA* **306**, 1574–1581 (2011).
91. National Heart, Lung, and Blood Institute Acute Respiratory Distress Syndrome (ARDS) Clinical Trials Network *et al.* Randomized, placebo-controlled clinical trial of an aerosolized β_2 -agonist for treatment of acute lung injury. *Am. J. Respir. Crit. Care Med.* **184**, 561–568 (2011).
92. Dellinger, R. P. *et al.* Effects of inhaled nitric oxide in patients with acute respiratory distress syndrome: results of a randomized phase II trial. Inhaled Nitric Oxide in ARDS Study Group. *Crit. Care Med.* **26**, 15–23 (1998).
93. Papazian, L. *et al.* Neuromuscular blockers in early acute respiratory distress syndrome. *N. Engl. J. Med.* **363**, 1107–1116 (2010).
94. Pacurari, M., Lowe, K., Tchounwou, P. B. & Kafoury, R. A Review on the Respiratory System Toxicity of Carbon Nanoparticles. *Int. J. Environ. Res. Public Health* **13**, (2016).
95. Kayat, J., Gajbhiye, V., Tekade, R. K. & Jain, N. K. Pulmonary toxicity of carbon nanotubes: a systematic report. *Nanomedicine Nanotechnol. Biol. Med.* **7**, 40–49 (2011).
96. Sayes, C. M. *et al.* The Differential Cytotoxicity of Water-Soluble Fullerenes. *Nano Lett.* **4**, 1881–1887 (2004).
97. Sayes, C. M. *et al.* Functionalization density dependence of single-walled carbon nanotubes cytotoxicity in vitro. *Toxicol. Lett.* **161**, 135–142 (2006).
98. Journeay, W. S., Suri, S. S., Moralez, J. G., Fenniri, H. & Singh, B. Rosette nanotubes show low acute pulmonary toxicity in vivo. *Int. J. Nanomedicine* **3**, 373–384 (2008).
99. Bonner, J. C. Carbon nanotubes as delivery systems for respiratory disease: do the dangers outweigh the potential benefits? *Expert Rev. Respir. Med.* **5**, 779–787 (2011).
100. Card, J. W., Zeldin, D. C., Bonner, J. C. & Nestmann, E. R. Pulmonary applications and toxicity of engineered nanoparticles. *Am. J. Physiol. - Lung Cell. Mol. Physiol.* **295**, L400–L411 (2008).
101. Hussain, S. *et al.* Multiwalled Carbon Nanotube Functionalization with High Molecular Weight Hyaluronan Significantly Reduces Pulmonary Injury. *ACS Nano* **10**, 7675–7688 (2016).

102. Shuvaev, V. V. & Muzykantov, V. R. Targeted modulation of reactive oxygen species in the vascular endothelium. *J. Control. Release Off. J. Control. Release Soc.* **153**, 56–63 (2011).
103. Howard, M. D., Greineder, C. F., Hood, E. D. & Muzykantov, V. R. Endothelial targeting of liposomes encapsulating SOD/Catalase mimetic EUK-134 alleviates acute pulmonary inflammation. *J. Control. Release Off. J. Control. Release Soc.* **177**, 34–41 (2014).
104. Manickam, D. S. *et al.* Well-defined cross-linked antioxidant nanozymes for treatment of ischemic brain injury. *J. Control. Release Off. J. Control. Release Soc.* **162**, 636–645 (2012).
105. Supinski, G. S. & Callahan, L. A. Polyethylene glycol-superoxide dismutase prevents endotoxin-induced cardiac dysfunction. *Am. J. Respir. Crit. Care Med.* **173**, 1240–1247 (2006).
106. Mitsopoulos, P. *et al.* Effectiveness of liposomal-N-acetylcysteine against LPS-induced lung injuries in rodents. *Int. J. Pharm.* **363**, 106–111 (2008).
107. Jaiswal, M., Dudhe, R. & Sharma, P. K. Nanoemulsion: an advanced mode of drug delivery system. *3 Biotech* **5**, 123–127 (2015).
108. Wagner, J. G., Gerard, E. S. & Kaiser, D. G. The effect of the dosage form on serum levels of indoxole. *Clin. Pharmacol. Ther.* **7**, 610–619 (1966).
109. Kim, C. K., Cho, Y. J. & Gao, Z. G. Preparation and evaluation of biphenyl dimethyl dicarboxylate microemulsions for oral delivery. *J. Control. Release Off. J. Control. Release Soc.* **70**, 149–155 (2001).
110. Hou, S. *et al.* Therapeutic Effect of Intravenous Infusion of Perfluorocarbon Emulsion on LPS-Induced Acute Lung Injury in Rats. *PLoS ONE* **9**, (2014).
111. David, D. R. Clinical manual of emergency psychiatry. *J. Forensic Psychiatry Psychol.* **22**, 310–311 (2011).
112. Pedersen, G. P., Fäldt, P., Bergenståhl, B. & Kristensen, H. G. Solid state characterisation of a dry emulsion: a potential drug delivery system. *Int. J. Pharm.* **171**, 257–270 (1998).

113. Cabrales, P., Vázquez, B. Y. S., Negrete, A. C. & Intaglietta, M. Perfluorocarbons as gas transporters for O₂, NO, CO and volatile anesthetics. *Transfus. Altern. Transfus. Med.* **9**, 294–303 (2007).
114. Riess, J. G. Oxygen carriers ('blood substitutes')--raison d'être, chemistry, and some physiology. *Chem. Rev.* **101**, 2797–2920 (2001).
115. Clark, L. C. & Gollan, F. Survival of mammals breathing organic liquids equilibrated with oxygen at atmospheric pressure. *Science* **152**, 1755–1756 (1966).
116. Lowe, K. C. Engineering blood: synthetic substitutes from fluorinated compounds. *Tissue Eng.* **9**, 389–399 (2003).
117. Janjic, J., Patel, S. K. & Faber, C. Chapter 14 Perfluorocarbon Theranostic Nanomedicines: Pharmaceutical Scientist's Perspective. in (2016). doi:10.1201/9781315364605-15.
118. Kabalnov, A. S. & Shchukin, E. D. Ostwald ripening theory: applications to fluorocarbon emulsion stability. *Adv. Colloid Interface Sci.* **38**, 69–97 (1992).
119. Sharts, C. M. *et al.* The solubility of oxygen in aqueous fluorocarbon emulsions. *J. Fluor. Chem.* **11**, 637–641 (1978).
120. Hsu, L.-C., Creech, J., Zalesky, P. & Kivinski, M. Perfluorocarbon emulsions with non-fluorinated surfactants. (2004).
121. Washington, C. & King, S. M. Effect of Electrolytes and Temperature on the Structure of a Poly(ethylene oxide)–Poly(propylene oxide)– Poly(ethylene oxide) Block Copolymer Adsorbed to a Perfluorocarbon Emulsion. *Langmuir* **13**, 4545–4550 (1997).
122. Washington, C. *et al.* Polymer Bristles: Adsorption of Low Molecular Weight Poly(oxyethylene)–Poly(oxybutylene) Diblock Copolymers on a Perfluorocarbon Emulsion. *Macromolecules* **33**, 1289–1297 (2000).
123. Meyer, K. L., Joseph, P. M., Mukherji, B., Livolsi, V. A. & Lin, R. Measurement of vascular volume in experimental rat tumors by ¹⁹F magnetic resonance imaging. *Invest. Radiol.* **28**, 710–719 (1993).

124. Mukherjee, B. *et al.* Chapter 7 - Multifunctional drug nanocarriers facilitate more specific entry of therapeutic payload into tumors and control multiple drug resistance in cancer. in *Nanobiomaterials in Cancer Therapy* (ed. Grumezescu, A. M.) 203–251 (William Andrew Publishing, 2016). doi:10.1016/B978-0-323-42863-7.00007-4.
125. Lim, S. B., Rubinstein, I., Sadikot, R. T., Artwohl, J. E. & Önyüksel, H. A Novel Peptide Nanomedicine Against Acute Lung Injury: GLP-1 in Phospholipid Micelles. *Pharm. Res.* **28**, 662–672 (2011).
126. Sadikot, R. T. & Rubinstein, I. Long-Acting, Multi-Targeted Nanomedicine: Addressing Unmet Medical Need in Acute Lung Injury. *J. Biomed. Nanotechnol.* **5**, 614–619 (2009).
127. *Nanomaterials: A Danger or a Promise?: A Chemical and Biological Perspective.* (Springer-Verlag, 2013). doi:10.1007/978-1-4471-4213-3.
128. Millar, F. R., Summers, C., Griffiths, M. J., Toshner, M. R. & Proudfoot, A. G. The pulmonary endothelium in acute respiratory distress syndrome: insights and therapeutic opportunities. *Thorax* **71**, 462–473 (2016).
129. Jules-Elysee, K. & White, D. A. Bleomycin-induced pulmonary toxicity. *Clin. Chest Med.* **11**, 1–20 (1990).
130. Patil, M. A. *et al.* Targeted delivery of YSA-functionalized and non-functionalized polymeric nanoparticles to injured pulmonary vasculature. *Artif. Cells Nanomedicine Biotechnol.* **46**, S1059–S1066 (2018).
131. Carpenter, T. C., Schroeder, W., Stenmark, K. R. & Schmidt, E. P. Eph-A2 promotes permeability and inflammatory responses to bleomycin-induced lung injury. *Am. J. Respir. Cell Mol. Biol.* **46**, 40–47 (2012).
132. Li, S. *et al.* Anti-ICAM-1 antibody-modified nanostructured lipid carriers: a pulmonary vascular endothelium-targeted device for acute lung injury therapy. *J. Nanobiotechnology* **16**, 105 (2018).

133. Villar, J. *et al.* Evaluating the efficacy of dexamethasone in the treatment of patients with persistent acute respiratory distress syndrome: study protocol for a randomized controlled trial. *Trials* **17**, 342 (2016).
134. Riyaz, B., Sudhakar, K. & Mishra, V. Quantum Dot-Based Drug Delivery for Lung Cancer. in *Nanotechnology-Based Targeted Drug Delivery Systems for Lung Cancer* 311–326 (Elsevier, 2019). doi:10.1016/B978-0-12-815720-6.00013-7.
135. Su, Y. *et al.* The cytotoxicity of cadmium based, aqueous phase - synthesized, quantum dots and its modulation by surface coating. *Biomaterials* **30**, 19–25 (2009).
136. Zhu, C. *et al.* Recent advances in non-toxic quantum dots and their biomedical applications. *Prog. Nat. Sci. Mater. Int.* **29**, 628–640 (2019).
137. Jha, A. *et al.* DNA biodots based targeted theranostic nanomedicine for the imaging and treatment of non-small cell lung cancer. *Int. J. Biol. Macromol.* **150**, 413–425 (2020).
138. Johari-Ahar, M. *et al.* Methotrexate-conjugated quantum dots: synthesis, characterisation and cytotoxicity in drug resistant cancer cells. *J. Drug Target.* **24**, 120–133 (2016).
139. Chakravarthy, K. V. *et al.* Doxorubicin conjugated quantum dots to target alveolar macrophages/inflammation. *Nanomed.* **7**, 88–96 (2011).
140. Hoshyar, N., Gray, S., Han, H. & Bao, G. The effect of nanoparticle size on in vivo pharmacokinetics and cellular interaction. *Nanomed.* **11**, 673–692 (2016).
141. Singh, R. & Lillard, J. W. Nanoparticle-based targeted drug delivery. *Exp. Mol. Pathol.* **86**, 215–223 (2009).
142. Zauner, W., Farrow, N. A. & Haines, A. M. In vitro uptake of polystyrene microspheres: effect of particle size, cell line and cell density. *J. Control. Release Off. J. Control. Release Soc.* **71**, 39–51 (2001).
143. Chen, K.-H. *et al.* Nanoparticle distribution during systemic inflammation is size-dependent and organ-specific. *Nanoscale* **7**, 15863–15872 (2015).

144. Albanese, A., Tang, P. S. & Chan, W. C. W. The Effect of Nanoparticle Size, Shape, and Surface Chemistry on Biological Systems. *Annu. Rev. Biomed. Eng.* **14**, 1–16 (2012).
145. Choi, H. S. *et al.* Renal Clearance of Nanoparticles. *Nat. Biotechnol.* **25**, 1165–1170 (2007).
146. Liu, X., Huang, N., Li, H., Jin, Q. & Ji, J. Surface and size effects on cell interaction of gold nanoparticles with both phagocytic and nonphagocytic cells. *Langmuir ACS J. Surf. Colloids* **29**, 9138–9148 (2013).
147. Dreaden, E. C., Austin, L. A., Mackey, M. A. & El-Sayed, M. A. Size matters: gold nanoparticles in targeted cancer drug delivery. *Ther. Deliv.* **3**, 457–478 (2012).
148. Elias, D. R., Poloukhine, A., Popik, V. & Tsourkas, A. Effect of ligand density, receptor density, and nanoparticle size on cell targeting. *Nanomedicine Nanotechnol. Biol. Med.* **9**, 194–201 (2013).
149. Standiford, T. J. & Ward, P. A. Therapeutic Targeting of Acute Lung Injury and ARDS. *Transl. Res. J. Lab. Clin. Med.* **167**, 183–191 (2016).
150. Takenaka, S. *et al.* Distribution pattern of inhaled ultrafine gold particles in the rat lung. *Inhal. Toxicol.* **18**, 733–740 (2006).
151. Thorley, A. J., Ruenraroengsak, P., Potter, T. E. & Tetley, T. D. Critical Determinants of Uptake and Translocation of Nanoparticles by the Human Pulmonary Alveolar Epithelium. *ACS Nano* **8**, 11778–11789 (2014).
152. Gratton, S. E. A. *et al.* The effect of particle design on cellular internalization pathways. *Proc. Natl. Acad. Sci.* **105**, 11613–11618 (2008).
153. Chithrani, B. D. & Chan, W. C. W. Elucidating the Mechanism of Cellular Uptake and Removal of Protein-Coated Gold Nanoparticles of Different Sizes and Shapes. *Nano Lett.* **7**, 1542–1550 (2007).
154. Hutter, E. *et al.* Microglial Response to Gold Nanoparticles. *ACS Nano* **4**, 2595–2606 (2010).
155. Lu, F., Wu, S.-H., Hung, Y. & Mou, C.-Y. Size effect on cell uptake in well-suspended, uniform mesoporous silica nanoparticles. *Small Weinh. Bergstr. Ger.* **5**, 1408–1413 (2009).
156. Lynch, I. & Dawson, K. A. Protein-nanoparticle interactions. *Nano Today* **3**, 40–47 (2008).

157. Owens, D. E. & Peppas, N. A. Opsonization, biodistribution, and pharmacokinetics of polymeric nanoparticles. *Int. J. Pharm.* **307**, 93–102 (2006).
158. Cedervall, T. *et al.* Understanding the nanoparticle-protein corona using methods to quantify exchange rates and affinities of proteins for nanoparticles. *Proc. Natl. Acad. Sci.* **104**, 2050–2055 (2007).
159. Attia, M. F., Anton, N., Wallyn, J., Omran, Z. & Vandamme, T. F. An overview of active and passive targeting strategies to improve the nanocarriers efficiency to tumour sites. *J. Pharm. Pharmacol.* **71**, 1185–1198 (2019).
160. Lambert, E. & Janjic, J. M. Multiple linear regression applied to predicting droplet size of complex perfluorocarbon nanoemulsions for biomedical applications. *Pharm. Dev. Technol.* **24**, 700–710 (2019).
161. Weichert, D. *et al.* A review of machine learning for the optimization of production processes. *Int. J. Adv. Manuf. Technol.* **104**, 1889–1902 (2019).
162. Köksal, G., Batmaz, İ. & Testik, M. C. A review of data mining applications for quality improvement in manufacturing industry. *Expert Syst. Appl.* **38**, 13448–13467 (2011).
163. Youssar, S., Bahtaoui, M., Jarmouni, Y. & Berrado, A. Clustering of Pharmaceutical products using Random Forest algorithm. in *Proceedings of the 12th International Conference on Intelligent Systems: Theories and Applications* 1–6 (ACM, 2018). doi:10.1145/3289402.3289511.
164. Grapentin, C., Barnert, S. & Schubert, R. Monitoring the Stability of Perfluorocarbon Nanoemulsions by Cryo-TEM Image Analysis and Dynamic Light Scattering. *PLoS ONE* **10**, (2015).
165. Krämer, W. *et al.* Rational manufacturing of functionalized, long-term stable perfluorocarbon-nanoemulsions for site-specific 19F magnetic resonance imaging. *Eur. J. Pharm. Biopharm.* **142**, 114–122 (2019).
166. Liu, L., Bagia, C. & Janjic, J. M. The First Scale-Up Production of Theranostic Nanoemulsions. *BioResearch Open Access* **4**, 218–228 (2015).

167. Janjic, J. M., Srinivas, M., Kadayakkara, D. K. K. & Ahrens, E. T. Self-delivering Nanoemulsions for Dual Fluorine-19 MRI and Fluorescence Detection. *J. Am. Chem. Soc.* **130**, 2832–2841 (2008).
168. Zhang, H. Eu-chelate anti-fibrin antibody-conjugated perfluorocarbon nanoparticles. in *Molecular Imaging and Contrast Agent Database (MICAD)* (National Center for Biotechnology Information (US), 2004).
169. Shi, G. & Coger, R. N. Use of perfluorocarbons to enhance the performance of perfused three-dimensional hepatic cultures. *Biotechnol. Prog.* **29**, 718–726 (2013).
170. Kim, H. Y. *et al.* Oxygen-Releasing Microparticles for Cell Survival and Differentiation Ability under Hypoxia for Effective Bone Regeneration. *Biomacromolecules* **20**, 1087–1097 (2019).
171. Yu, P. *et al.* Artificial Red Blood Cells Constructed by Replacing Heme with Perfluorodecalin for Hypoxia-Induced Radioresistance. *Adv. Ther.* **2**, 1900031 (2019).
172. Tyssebotn, I. M., Lundgren, C. E. G., Olszowka, A. J. & Bergoe, G. W. Hypoxia Due to Shunts in Pig Lung Treated with O₂ and Fluorocarbon-derived Intravascular Microbubbles. *Artif. Cells Blood Substit. Biotechnol.* **38**, 79–89 (2010).
173. Zhou, Z. *et al.* Two-stage oxygen delivery for enhanced radiotherapy by perfluorocarbon nanoparticles. *Theranostics* **8**, 4898–4911 (2018).
174. Zhuang, J. *et al.* Biomimetic Nanoemulsions for Oxygen Delivery In Vivo. *Adv. Mater.* **30**, 1804693 (2018).
175. Rifai, N. A. *et al.* Ultrasound-triggered delivery of paclitaxel encapsulated in an emulsion at low acoustic pressures. *J. Mater. Chem. B* **8**, 1640–1648 (2020).
176. Prato, M. *et al.* 2H,3H-Decafluoropentane-Based Nanodroplets: New Perspectives for Oxygen Delivery to Hypoxic Cutaneous Tissues. *PLOS ONE* **10**, e0119769 (2015).
177. Sawdon, A. & Peng, C.-A. Internal deoxygenation of tubular photobioreactor for mass production of microalgae by perfluorocarbon emulsions. *J. Chem. Technol. Biotechnol.* **90**, 1426–1432 (2015).

178. Yao, Y. *et al.* Perfluorocarbon-Encapsulated PLGA-PEG Emulsions as Enhancement Agents for Highly Efficient Reoxygenation to Cell and Organism. *ACS Appl. Mater. Interfaces* **7**, 18369–18378 (2015).
179. Arnaud, F., Sanders, K., Sieckmann, D. & Moon-Massat, P. In vitro alteration of hematological parameters and blood viscosity by the perfluorocarbon: Oxycyte. *Int. J. Hematol.* **103**, 584–591 (2016).
180. Song, X., Feng, L., Liang, C., Yang, K. & Liu, Z. Ultrasound Triggered Tumor Oxygenation with Oxygen-Shuttle Nanoperfluorocarbon to Overcome Hypoxia-Associated Resistance in Cancer Therapies. *Nano Lett.* **16**, 6145–6153 (2016).
181. Song, G. *et al.* TaOx decorated perfluorocarbon nanodroplets as oxygen reservoirs to overcome tumor hypoxia and enhance cancer radiotherapy. *Biomaterials* **112**, 257–263 (2017).
182. Liu, Z. *et al.* Imaging assessment of cardioprotection mediated by a dodecafluoropentane oxygen-carrier administered during myocardial infarction. *Nucl. Med. Biol.* **70**, 67–77 (2019).
183. Day, R. A., Estabrook, D. A., Logan, J. K. & Sletten, E. M. Fluorous photosensitizers enhance photodynamic therapy with perfluorocarbon nanoemulsions. *Chem. Commun.* **53**, 13043–13046 (2017).
184. Cheng, Y. *et al.* Perfluorocarbon nanoparticles enhance reactive oxygen levels and tumour growth inhibition in photodynamic therapy. *Nat. Commun.* **6**, 8785 (2015).
185. Gulino, G. R. *et al.* Oxygen-Loaded Nanodroplets Effectively Abrogate Hypoxia Dysregulating Effects on Secretion of MMP-9 and TIMP-1 by Human Monocytes. *Mediators Inflamm.* **2015**, 1–11 (2015).
186. Mountain, G. A., Jelier, B. J., Bagia, C., Friesen, C. M. & Janjic, J. M. Design and formulation of nanoemulsions using 2-(poly(hexafluoropropylene oxide)) perfluoropropyl benzene in combination with linear perfluoro(polyethylene glycol dimethyl ether). *J. Fluor. Chem.* **162**, 38–44 (2014).
187. Neveu, M.-A. *et al.* Lactate Production Precedes Inflammatory Cell Recruitment in Arthritic Ankles: an Imaging Study. *Mol. Imaging Biol.* **22**, 1324–1332 (2020).

188. Rho, J. *et al.* Paramagnetic Fluorinated Nanoemulsions for in vivo F-19 MRI. 10.
189. Janjic, J. M. *et al.* Perfluorocarbon nanoemulsions with fluorescent, colloidal and magnetic properties. *Biomaterials* **35**, 4958–4968 (2014).
190. Hansson, K., Yella, S., Dougherty, M. & Fleyeh, H. Machine Learning Algorithms in Heavy Process Manufacturing. *Am. J. Intell. Syst.* **6**, 1–13 (2016).
191. Lingitz, L. *et al.* Lead time prediction using machine learning algorithms: A case study by a semiconductor manufacturer. *Procedia CIRP* **72**, 1051–1056 (2018).
192. Wu, L., Xiao, Y., Ghosh, M., Zhou, Q. & Hao, Q. Machine Learning Prediction for Bandgaps of Inorganic Materials. *ES Mater. Manuf.* **Volume 9**, 34–39 (2020).
193. Kuhn, M. & Johnson, K. *Applied Predictive Modeling*. (Springer-Verlag, 2013). doi:10.1007/978-1-4614-6849-3.
194. K. Gurpret & S. K. Singh. Review of Nanoemulsion Formulation and Characterization Techniques. *Indian J. Pharm. Sci.* **80**, (2018).
195. Honary, S. & Zahir, F. Effect of Zeta Potential on the Properties of Nano-Drug Delivery Systems - A Review (Part 1). *Trop. J. Pharm. Res.* **12**, 255–264 (2013).
196. Baboota, S., Shakeel, F., Ahuja, A., Ali, J. & Shafiq, S. Design, development and evaluation of novel nanoemulsion formulations for transdermal potential of celecoxib. *Acta Pharm. Zagreb Croat.* **57**, 315–332 (2007).
197. Sheth, T., Seshadri, S., Prileszky, T. & Helgeson, M. E. Multiple nanoemulsions. *Nat. Rev. Mater.* **5**, 214–228 (2020).
198. Herneisey, M. *et al.* Quality by Design Approach Using Multiple Linear and Logistic Regression Modeling Enables Microemulsion Scale Up. *Molecules* **24**, (2019).
199. Lambert, E. & Janjic, J. M. Quality by design approach identifies critical parameters driving oxygen delivery performance in vitro for perfluorocarbon based artificial oxygen carriers. *Sci. Rep.* **11**, 5569 (2021).